# *Fast*TIMES

## Seismic Methods:

### Secondary Effects of Voids on Seismic Waves

### Interpretation of Seismic Tomography Results Using Data Quality and Residual Error Maps

### Application of Shallow Seismic Refraction for Determining Geotechnical Properties and Competence of Karstic Limestone Bedrock in an Area West of Assiut, Egypt

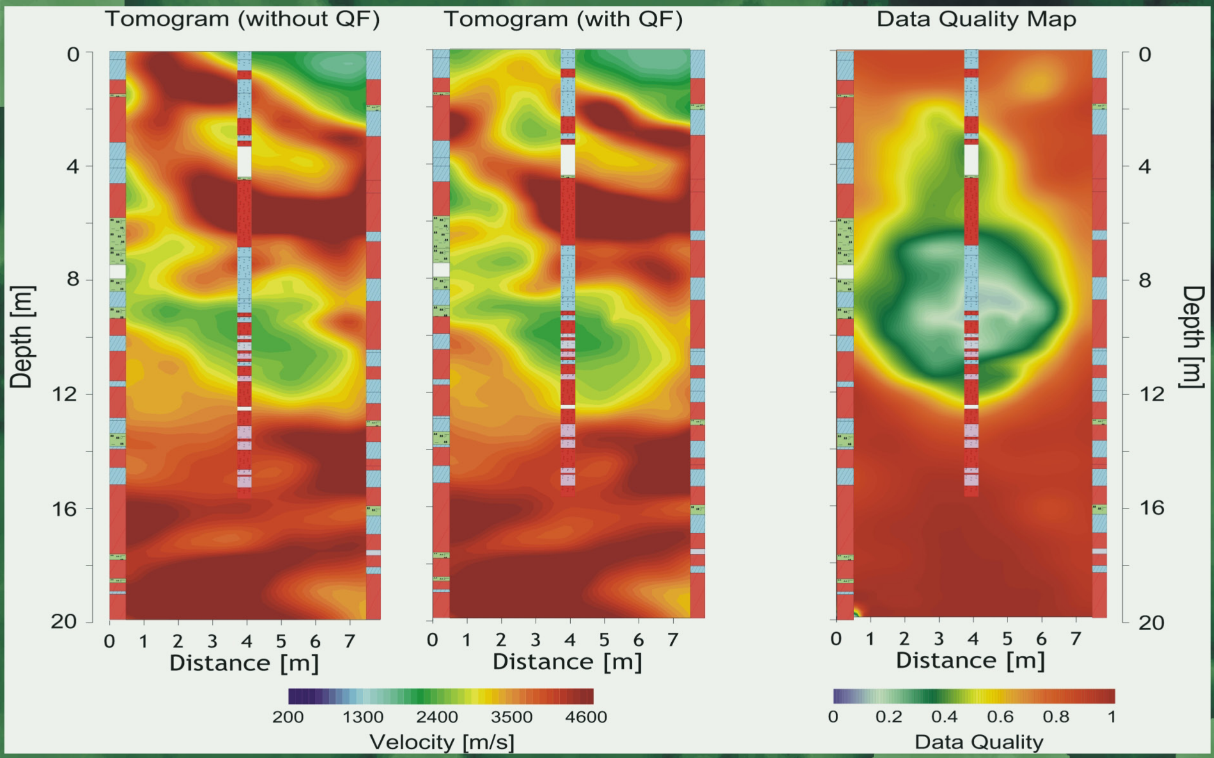


## Capacitatively-Coupled Resistivity:

### Tunnel Discrimination Using Mobile Geophysical Arrays


June 2014

Volume 19, Number 2

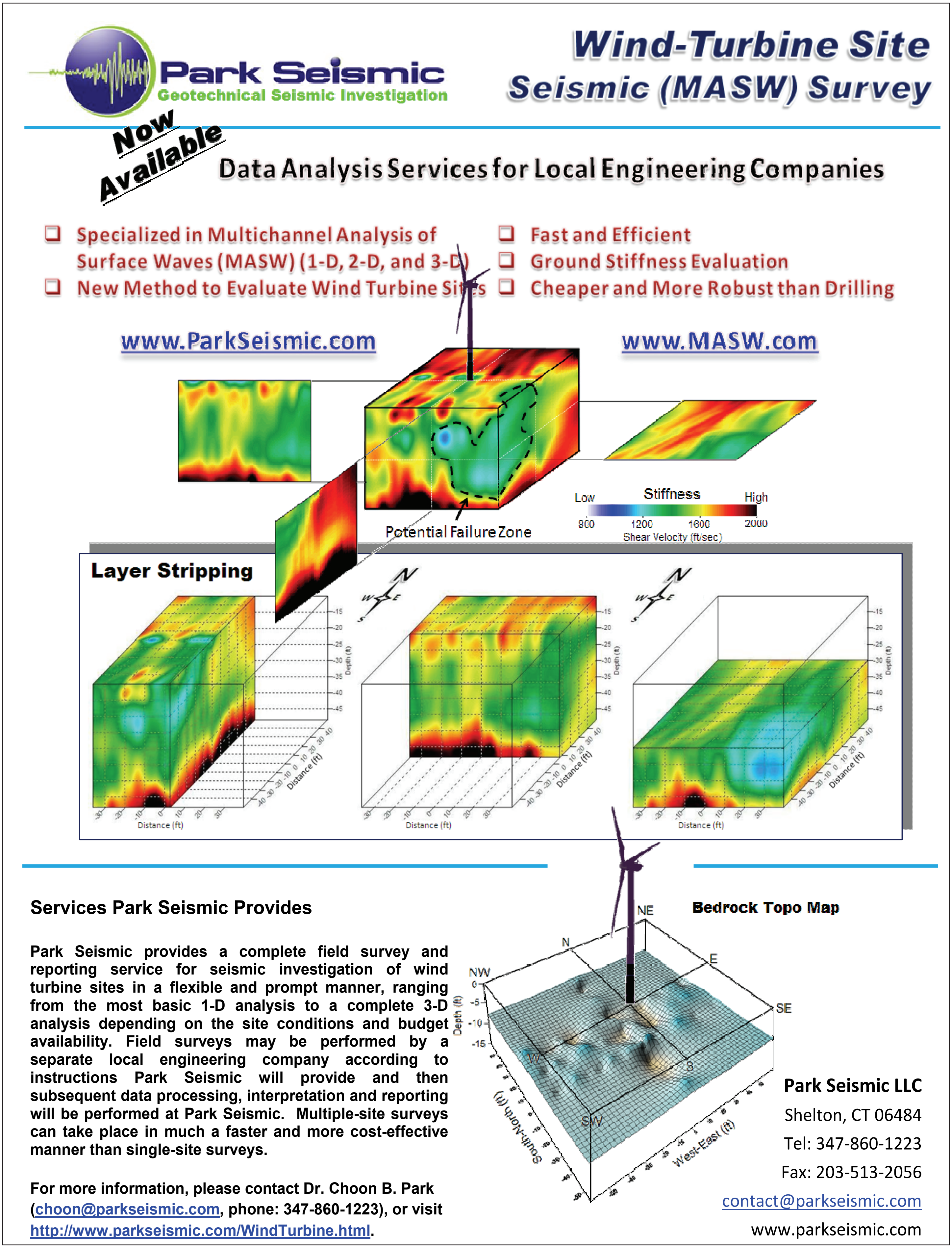
Park Seismic
Geotechnical Seismic Investigation
Wind-Turbine Site
Seismic (MASW) Survey
Now Available
Data Analysis Services for Local Engineering Companies
Specialized in Multichannel Analysis of Surface Waves (MASW) (1-D, 2-D, and 3-D)
New Method to Evaluate Wind Turbine Sites
Fast and Efficient
Ground Stiffness Evaluation
Cheaper and More Robust than Drilling
www.ParkSeismic.com
www.MASW.com
Potential Failure Zone
Low
Stiffness
High
800
1200
1600
2000
Shear Velocity (ft/sec)
Layer Stripping
Depth (ft)
Distance (ft)
Services Park Seismic Provides
Park Seismic provides a complete field survey and reporting service for seismic investigation of wind turbine sites in a flexible and prompt manner, ranging from the most basic 1-D analysis to a complete 3-D analysis depending on the site conditions and budget availability. Field surveys may be performed by a separate local engineering company according to instructions Park Seismic will provide and then subsequent data processing, interpretation and reporting will be performed at Park Seismic. Multiple-site surveys can take place in much a faster and more cost-effective manner than single-site surveys.
For more information, please contact Dr. Choon B. Park (choon@parkseismic.com, phone: 347-860-1223), or visit http://www.parkseismic.com/WindTurbine.html.
Bedrock Topo Map
NE
N
E
NW
SE
W
S
SW
Depth (ft)
South-North (ft)
West-East (ft)
Park Seismic LLC
Shelton, CT 06484
Tel: 347-860-1223
Fax: 203-513-2056
contact@parkseismic.com
www.parkseismic.com

In this issue, there are three seismic geophysics articles, one on underground void detection, a second on enhanced inversion for borehole tomography, and a third on the use of refraction techniques for geotechnical evaluation of karstic limestone bedrock. Furthermore, a fourth article is focused on tunnel discrimination using a capacitively-coupled resistivity (CCR) array and electrical resistivity tomography (ERT).

# Contents



## Advertisers



## Articles

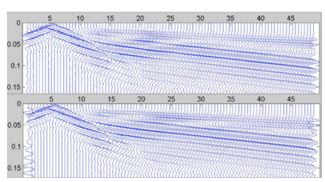

# *Fast*TIMES

*Fast*TIMES (ISSN 1943-6505) is published by the Environmental and Engineering Geophysical Society (EEGS). It is available electronically (as a pdf document) from the EEGS website (www.eegs.org).

## ABOUT EEGS

The Environmental and Engineering Geophysical Society (EEGS) is an applied scientific organization founded in 1992. Our mission:

*"To promote the science of geophysics especially as it is applied to environmental and engineering problems; to foster common scientific interests of geophysicists and their colleagues in other related sciences and engineering; to maintain a high professional standing among its members; and to promote fellowship and cooperation among persons interested in the science."*

We strive to accomplish our mission in many ways, including (1) holding the annual Symposium on the Application of Geophysics to Engineering and Environmental Problems (SAGEEP); (2) publishing the Journal of Environmental & Engineering Geophysics (JEEG), a peer-reviewed journal devoted to near-surface geophysics; (3) publishing *Fast*TIMES, a magazine for the near-surface community, and (4) maintaining relationships with other professional societies relevant to near-surface geophysics.

## JOINING EEGS

EEGS welcomes membership applications from individuals (including students) and businesses. Annual dues are $90 for an individual membership, $50 for introductory membership, $50 for a retired member, $50 developing world membership, complimentary corporate sponsored student membership - if available, and $300 to $4000 for various levels of corporate membership. All membership categories include free on-line access to JEEG. The membership application is available at the back of this issue, or online at www.eegs.org.



## HEAD OFFICE

1720 South Bellaire, Suite 110
Denver, Colorado 80222-4303;
PH 303.531.751, FX 303.820.3844
staff@eegs.org

Executive Director
Kathie A. Barstnar
staff@eegs.org

Managing Director
Jackie Jacoby
staff@eegs.org

## CONTRIBUTORS



## SUBMISSIONS

To submit information for inclusion in *Fast*TIMES, contact a member of the editorial team:

Editor in Chief
Barry Allred
Barry.Allred@ars.usda.gov
614.292.4459

Associate Editor
Moe Momayez
moe.momayez@arizona.edu
520.621.6580

Associate Editor
Jeffrey G. Paine
jeff.paine@beg.utexas.edu
512.471.1260

To advertise in FastTIMES, contact:

Jackie Jacoby
staff@eegs.org
303.531.7517

*Fast*TIMES is published electronically four times a year. Please send articles to any member of the editorial team by September 1, 2014. Advertisements are due to Jackie Jacoby by September 1, 2014.

# CALENDAR

## 2014

| | |
|---|---|
| August 24 - 30 | 22nd EM Induction Workshop<br>Weimar, Germany<br>http://www.emiw2014.de |
| September 30 | Agricultural Geophysics Webinar Series<br>"Using Ground Penetrating Radar for Agriculture"<br>http://www.ag-geophysics.org<br>(Note: See page 60 for additional information.) |
| October 26 - 31 | Society of Exploration Geophysicists International Exposition and 84th Annual Meeting<br>Denver, Colorado, USA<br>http://www.seg.org |
| November 6-7 | Multichannel Analysis of Surface Wave (MASW) Workshop<br>Lawrence, Kansas, USA<br>http://www.kgs.ku.edu/software/surfseis/workshops.html |
| December 3 - 4 | 1st Society of Exploration Geophysicists - Sociedade Brasileira de Geofísica Workshop on Near Surface Geophysics<br>Salvador, Brazil<br>http://www.seg.org/events/upcoming-seg-meetings/salvador2014 |
| December 15 - 19 | American Geophysical Union Fall Meeting<br>San Francisco, California, USA<br>http://fallmeeting.agu.org/2014/ |

## 2015

| | |
|---|---|
| February 15 - 18 | Australian Society of Exploration Geophysics and Petroleum Exploration Society of Australia - 24th International Geophysics Conference and Exhibition<br>Perth, Australia<br>http://www.conference.aseg.org.au<br>(Note: See page 60 for additional information.) |
| March 22 - 26 | Symposium on the Application of Geophysics to Engineering and Environmental Problems (SAGEEP)<br>Austin, Texas, USA<br>http://www.eegs.org/Annual-Meeting-SAGEEP/SAGEEP-2015<br>(Note: See page 59 for additional information.) |

Please send event listings, corrections or omitted events to any member of the *Fast*TIMES editorial team.

# NOTES FROM EEGS

## PRESIDENT'S MESSAGE

**Moe Momayez, President**
(mmomayez@email.arizona.edu)

INTO THE FUTURE

I am happy to report that EEGS has begun a significant renewal process. Looking back over 20 years of our society's leadership in the near-surface geophysics community and the recognition of our flagship conference SAGEEP, one cannot help but notice that we have been operating by relying on a somewhat dated business model. We are now conducting a deep review of our mission statement and business processes, from administration, to membership, publication, education, finance, and inter-societal relationships. I expect the review process to continue well into the fall season. Feel free to contact our administrative offices to share any ideas you may have that will help us improve the range and quality of services we provide to you.

Renewal also means new blood. We are investing a significant portion of our resources to build a strong membership base around student societies. We are also actively recruiting new members from the much larger community of professionals who are not trained geophysicists, but use geophysics every day to obtain a more detailed understanding of the subsurface processes and properties. We will continue to strengthen our existing connections and create new relationships with other societies.

The focal point of our future activities will be our presence on the worldwide web. Our website was completely revamped in 2011. It has become a much more user-friendly site, packed with resources and up-to-date information about events and developments in our field. Moving forward, the website will undergo additional transformations in functionality to include educational materials, webinars, and tools to improve membership benefits and better serve the near-surface community in general. We are preparing an attractive marketing package for our corporate members that will maximize their advertising dollars.

The challenges EEGS has faced in the past 18 months have done nothing to deter us from forging ahead and building a stronger society. In point of fact, the SAGEEP 2015 organizing committee is already executing a plan that is well on track to bring you the best SAGEEP ever. Our conference will take place from March 22 to 26 in the vibrant city center of Austin, Texas. For those of you who are festival enthusiasts, SAGEEP is scheduled the week after the renowned South by Southwest (SXSW) Festival. The SAGEEP hotel special rate will include 3 days prior to SAGEEP. I hope you make early plans to attend this iconic Austin spring film and music event, as well as join me at SAGEEP 2015. Looking forward to seeing you all,

Moe Momayez, EEGS President

## EEGS Foundation makes great strides in its first years.

Since the launch of the EEGS Foundation, there are numerous accomplishments for which we can all be proud: Establishing and organizing a structure that serves the needs of EEGS; underwriting the legal process, achieving tax-exempt status; and soliciting and receiving support for SAGEEP. In addition, the Foundation helped underwrite the SAGEEP conference held this spring in Keystone.

These are only a few of the tangible results your donations to the Foundation have enabled. We would therefore like to recognize and gratefully thank the following individuals and companies for their generous contributions:

Allen, Micki
Arumugam, Devendran
Astin, Timothy
Baker, Gregory
Barkhouse, William
Barrow, Bruce
Billingsley, Patricia
Blackey, Mark
Brown, Bill
Butler, Dwain
Butler, Karl
Campbell, Kerry
Clark, John
Doll, William
Dunbar, John
Dunscomb, Mark
Greenhouse, John
Harry, Dennis
Holt, Jennifer
Ivanov, Julian
Jacobs, Rhonda
Kerry Campbell
Kimball, Mindy
Kruse, Sarah
LaBrecque, Douglas
Lecomte, Isabelle
Long, Leland
Lucius, Jeff
Luke, Barbara
MacInnes, Scott
Malkov, Mikhail
Markiewicz, Richard
Mills, Dennis
Momayez, Moe
Nazarian, Soheil
Nicholl, John
Nyquist, Jonathan
Paine, Jeffrey
Pullan, Susan
Rix, Glenn
Simms, Janet
Skokan, Catherine
Smith, Bruce
Soloyanis, Susan
Stowell, John
Strack, Kurt
Thompson, Michael
Tsoflias, George
Van Hollebeke, Philip
Yamanaka, Hiroaki

Adaptive Technical Solutions LLC
Corona Resources
Exploration Instruments LLC
Mt. Sopris Instruments

***"Guiding Technologies Today -Preparing for a World of Needs Tomorrow"***

# NOTES FROM EEGS

## Renew your EEGS Membership for 2014

Be sure to renew your EEGS membership for 2014! In addition to the more tangible member benefits (including the option of receiving a print or electronic subscription to JEEG, *Fast*TIMES delivered to your email box quarterly, discounts on EEGS publications and SAGEEP registration, and benefits from associated societies), your dues help support EEGS's major initiatives such as producing our annual meeting (SAGEEP), publishing JEEG, making our publications available electronically, expanding the awareness of near-surface geophysics outside our discipline, and enhancing our web site to enable desired capabilities such as membership services, publication ordering, and search and delivery of SAGEEP papers. You will also have the opportunity to donate to the EEGS Foundation during the renewal process. Members can renew by mail, fax, or online at www.eegs.org.

## Sponsorship Opportunities

There are always sponsorship opportunities available for government agencies, corporations, and individuals who wish to help support EEGS's activities. Specific opportunities include development and maintenance of an online system for accessing SAGEEP papers from the EEGS web site and support for our next SAGEEP. Make this the year your company gets involved! Contact Moe Momayez (mmomayez@email.arizona.edu) for more information.

# From the *Fast*TIMES Editorial Team

*Fast*TIMES is distributed as an electronic document (pdf) to all EEGS members, sent by web link to several related professional societies, and is available to all for downloading from the EEGS *Fast*TIMES web site ( http://www.eegs.org/Publications-Merchandise/FASTTIMES ). Past issues of *Fast*TIMES continually rank among the top downloads from the EEGS web site. Your articles, advertisements, and announcements receive a wide audience, both within and outside the geophysics community.

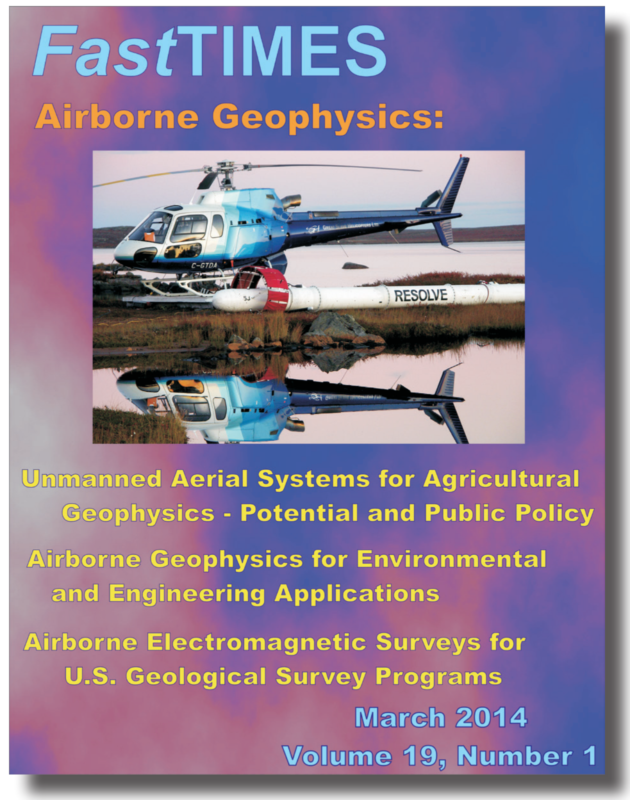


To keep the content of *Fast*TIMES fresh, the editorial team strongly encourages submissions from researchers, instrument makers, software designers, practitioners, researchers, and consumers of geophysics—in short, everyone with an interest in near-surface geophysics, whether you are an EEGS member or not. We welcome short research articles or descriptions of geophysical successes and challenges, summaries of recent conferences, notices of upcoming events, descriptions of new hardware or software developments, professional opportunities, problems needing solutions, and advertisements for hardware, software, or staff positions.

The *Fast*TIMES presence on the EEGS web site has been redesigned. At http://www.eegs.org/Publications-Merchandise/FASTTIMES you'll now find calls for articles, author guidelines, current and past issues, and advertising information.

## Submissions

The *Fast*TIMES editorial team welcomes contributions of any subject touching upon geophysics. *Fast*TIMES also accepts photographs and brief non-commercial descriptions of new instruments with possible environmental or engineering applications, news from geophysical or earth-science societies, conference notices, and brief reports from recent conferences. Please submit your items to a member of the *Fast*TIMES editorial team by September 1 to ensure inclusion in the next issue. We look forward to seeing your work in our pages. Note: Plans are for the September *Fast*TIMES issue to focus on geophysical methods used for locating UXO, and submission of short articles and case histories on this topic are highly encouraged. The December FastTIMES issue will highlight EEGS student chapters.

The Journal of Environmental & Engineering Geophysics (JEEG), published four times each year, is the EEGS peer-reviewed and Science Citation Index (SCI®)-listed journal dedicated to near-surface geophysics. It is available in print by subscription, and is one of a select group of journals available through GeoScienceWorld (www.geoscienceworld.org). JEEG is one of the major benefits of an EEGS membership. Information regarding preparing and submitting JEEG articles is available at http://jeeg.allentrack.net.

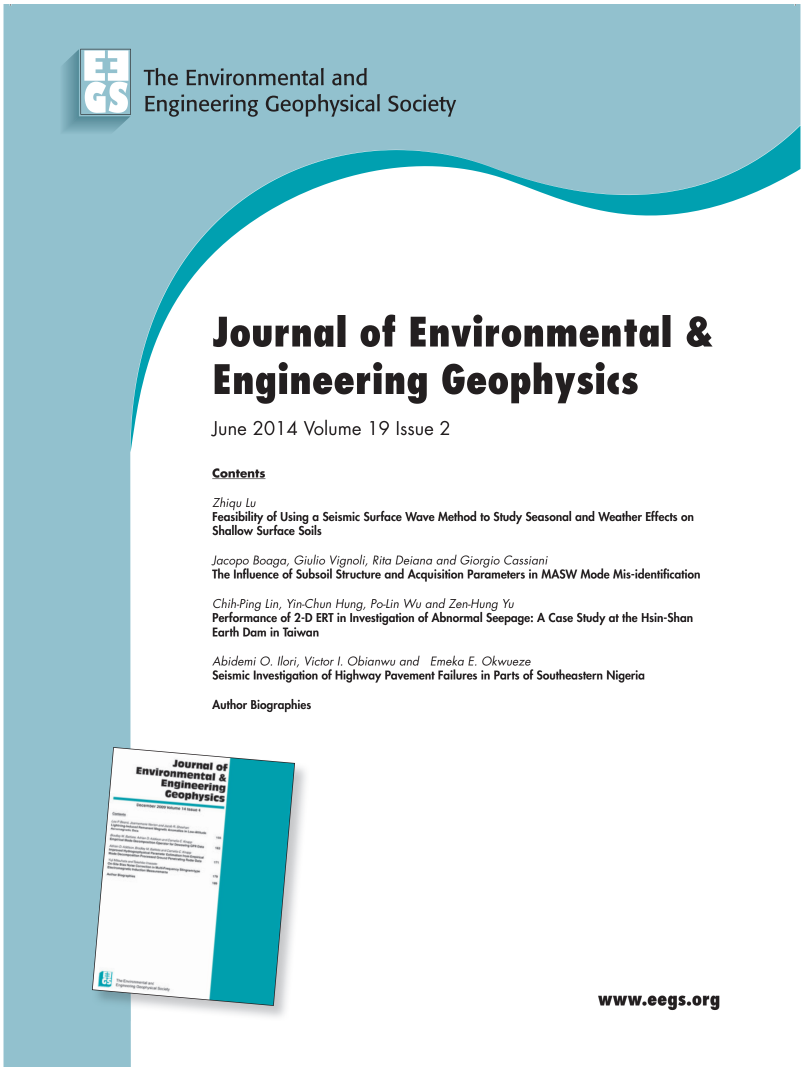


**June 2014 Volume 19 Issue 2**



# Editor's Note

Dr. Janet E. Simms
JEEG Editor-in-Chief
US Army Engineer R&D Ctr.
3909 Halls Ferry Road
Vicksburg, MS 39180-6199
(601) 634-3493; 634-3453 fax
janet.e.simms@erdc.usace.army.mil

The Journal of Environmental and Engineering Geophysics (JEEG) is the flagship publication of the Environmental and Engineering Geophysical Society (EEGS). All topics related to geophysics are viable candidates for publication in JEEG, although its primary emphasis is on the theory and application of geophysical techniques for environmental, engineering, and mining applications. There is no page limit, and no page charges for the first ten journal pages of an article. The review process is relatively quick; articles are often published within a year of submission. Articles published in JEEG are available electronically through GeoScienceWorld and the SEG's Digital Library in the EEGS Research Collection. Manuscripts can be submitted online at www.eegs.org/Publications-Merchandise/JEEG.

# SUPPORT EEGS TODAY

## JOIN OR RENEW
## SUBMIT AN ARTICLE
## GET INVOLVED!

## START HERE.

EEGS

www.eegs.org

# SUCCESS WITH GEOPHYSICS

FastTIMES welcomes short articles on applications of geophysics to the near surface in many disciplines, including engineering and environmental problems, geology, hydrology, agriculture, archaeology, and astronomy. In this issue, there are three seismic geophysics articles, one on underground void detection, a second on enhanced inversion for borehole tomography, and a third on the use of refraction techniques for geotechnical evaluation of karstic limestone bedrock. Furthermore, a fourth article is focused on tunnel discrimination using a capacitatively-coupled resistivity (CCR) array and electrical resistivity tomography (ERT).

# SECONDARY EFFECTS OF VOIDS ON SEISMIC WAVES

**Nedra D. Bonal, Ph.D., Geophysicist**
**Geophysics and Atmospheric Sciences Dept.**
**Sandia National Laboratories**
**PO Box 5800, Mail Stop 0750**
**Albuquerque, New Mexico 87185-0750**
**email: nbonal@sandia.gov**

**Sharon Desilets, Ph.D., Hydrologist**
**Consultant**
**1316 Wellesley Drive, NE**
**Albuquerque, New Mexico 87106**
**email: seinloth@gmail.com**

## Introduction

Detecting underground voids with seismic data is difficult. Seismic waves tend to go around the void. Little information from the void is returned to receivers at the surface. Therefore, refraction and reflection techniques that rely on wave interactions at the air-rock boundary are often unsuccessful at detecting voids. Changes in the rock produced by the void may contribute to this effect. Formation of the void produces fractures in the rock, affects stress locally, and changes the water content in the pores near the void. We model the impact of these effects on seismic waves to determine their influence on void detection.

## Methods

Pore saturation due to voids is modeled using vadose zone hydrology software. Results of the hydrology modeling are used as inputs to wave propagation code to simulate seismic waves through the model. The results of the simulation are then used to determine the impact that changes in the rock due to the void have on seismic waves.

Three models of the void relative to the water table are considered: a tunnel in the vadose zone far above the water table, a tunnel in the vadose zone close to the water table, and a tunnel in the saturated zone below the water table. Additionally, a “halo” region around the tunnel is considered for each model to represent saturation, fracture, and stress changes due to the void itself. This halo region was modeled with higher fluid conductivity to account for changes in fracturing and stress in addition to the hydrology effects of saturation changes. This results in six different models.

***Keywords:*** Void Detection, Seismic Modeling, Hydrologic Effects, Fluid Substitutions.

### Hydrology Modeling

The top and side boundary conditions are the same for each of the three models relative to the water table. The boundary at the top of the domain is atmospheric, which allows for a prescribed time-variable schedule of precipitation and evaporation. The sides of the domain are zero flux. The bottom boundary is set to free drainage for the unsaturated model with the deep water table and to constant pressure head for the two vadose zone models where the tunnel is above the water table. The tunnel boundary is a seepage face, a system-dependent condition that sets the boundary to a constant head of zero when saturated, and zero flux when unsaturated. The code assumes that water crossing the boundary is immediately removed from the system (e.g. in this model by pumping from the tunnel). The dimensions and boundary conditions of the hydrology model with the tunnel are shown in Figure 1A.

A three-layer model is used with the tunnel in a clay loam layer to maximize the effects of the hydrology around the void. A region of higher fluid conductivity, the "halo", representing increased fracturing and decreased stress surrounds the tunnel void and gradually diminishes into the rock. A finite element mesh is used in the hydrology model, which has finer resolution in the area of the tunnel. The finite element mesh of the model is shown in Figure 1B.

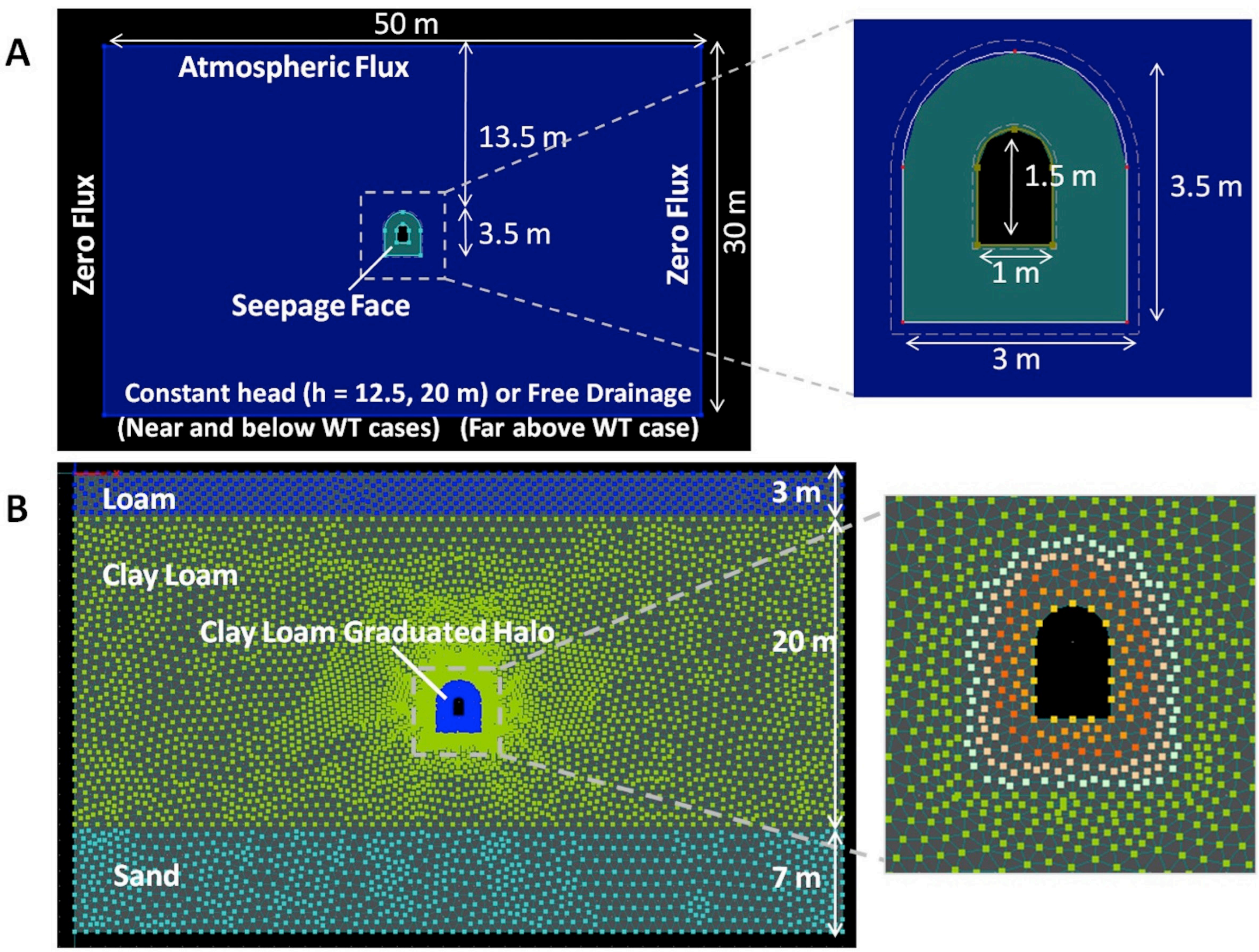


**Figure 1:** Model domain showing (**A**) dimensions and boundary conditions of the hydrology model, and (**B**) the finite element mesh with a fine-mesh, high-conductivity halo area around void, and three material layers. The colored nodes in the high-conductivity halo area show the graduated assignment of properties, moving from a coarse-fractured medium at the void edge to background values for surrounding medium.

### Seismic Velocity Determination

Hydrology results of water content are converted into P-wave velocities using one of two fluid substitution methods. The method by Brutsaert (1964) is used for weaker materials and the Biot-Gassmann (1956 and 1951, respectively) relation is used for stronger, deeper materials. We apply Brutsaert's equations to all soil with depth less than 5 m, and also to the high conductivity halo around the void. Brutsaert's equations best estimate velocities where capillary suction is significant relative to overburden pressure. The Biot-Gassmann equations are used everywhere else in the model.

### Synthetic Seismic Wave Propagation

Input for the seismic propagation code includes P-wave velocity (Vp), shear-wave velocity (Vs), and density (ρ). Vp was obtained from the water content results from the hydrology models described above. These results are expanded in one dimension to create a pseudo-3D volume. Vs is obtained by multiplying the values in Vp by 0.4, which is typically used to represent near surface velocities. Density, ρ, is obtained using the standard Gardner's relation (Gardner et al., 1974), $\rho = \alpha * Vp^{\beta}$, where ρ is in $kg/m^3$, $\alpha = 0.31$, and $\beta = 0.25$.

The synthetic seismic data are modeled to represent a linear refraction style survey with source locations spaced every 5 m along the ground surface of the modeled space from 5 m to 45 m. Source locations at 2 m and 48 m are also collected to get data at far offsets and spacing is reduced to 1 m between 20 m and 30 m to increase resolution near the tunnel. Three component receivers are spaced at 0.5 m intervals starting at 1.25 m and ending at 48.75 m and are buried 1 m below the ground surface to decrease noise. This configuration prevented sources from being located on top receivers.

## Results

### Hydrology Modeling

Results have been calculated for each of the three models relative to the water table, considering a tunnel with and without a halo region of increased hydraulic conductivity for a total of 6 models. For each model, the presence of the tunnel changes the flow pattern and water content in the surrounding material. The presence of the high-conductivity halo increases the size of the area of influence around the void. Additionally, for models where the tunnel is below the water table, the tunnel acts as a drain to locally depress the water table. The area of influence where the water table is drawn down due to draining through the tunnel is many times larger than the tunnel itself. These changes result in a larger footprint than the void, creating a larger target for the seismic waves. Details of the hydrology modeling can be found in Bonal and Desilets (in progress).

### Seismic Velocity

Seismic velocity is determined for all models described above. The velocity differences are bi-modally distributed: the variations in the halo region affect a larger velocity difference due to material differences (lower bulk modulus) while, outside of the halo region, the differences result from changes in water content and are three orders of magnitude smaller. For the far above water table model without a high-conductivity halo (Figure 2, top row, left column), the area affected by the tunnel is 9 times larger than the tunnel itself when including the small-scale effects. For the above water table model with the tunnel surrounded by a high-conductivity halo (Figure 2, top row, right column), the halo region shows much greater velocity change (65%). The halo itself triples the areal extent of higher-order velocity change. The lower-order effects increase the total footprint by 54 times the size of the tunnel.

The results for the tunnel above a near water table (Figure 2, middle row) are similar in pattern to that of the far above model. The proximity of the water table does not significantly change the areal extent of the velocity-disturbance footprint. However, the water table here does obscure the region of slight velocity change below the tunnel present in the previous model.

For the model where the tunnel is located below the water table (Figure 2, bottom row), pumping water from the tunnel draws down the water table over the tunnel. The drained region shows the most significant higher-order changes in velocity due to the large change in water content. The size of this effect would increase as the depth of the tunnel below the water table increases. The halo region still shows significant velocity changes as well, with the greatest change (69%) occurring in the part of the halo above and beside the tunnel.

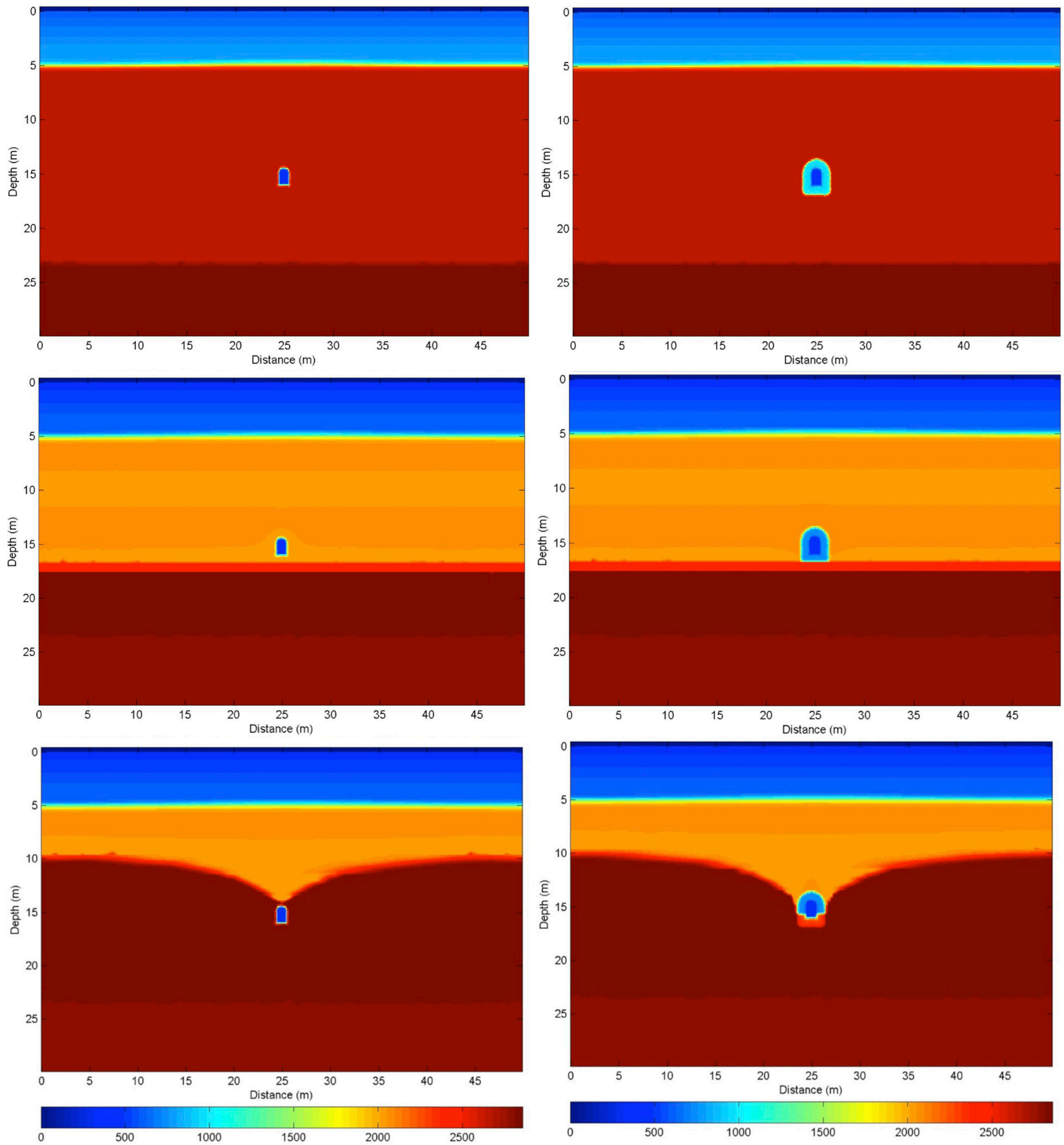


**Figure 2:** Seismic velocity results. The tunnel is far above (top row), near (middle row), and below (bottom row) the water table. The left column does not include a halo representing higher fluid conductivity. The right column contains models a halo around the void. The scale at the bottom of each column is P-wave velocity in m/s.

### Synthetic Seismic Waves

The presence of the tunnel above the water table without the halo has relatively minor effects on the amplitude and waveform character of the seismic waves compared to no tunnel present. The presence of the halo slightly alters the amplitudes of the waves at near offsets and alters the character of the waveform after the wave passes the tunnel location. Example shot gathers for the far above water table model is shown in Figure 3. For the below water table model (Figure 2, bottom), pumping water out of the tunnel draws down the water table locally above the tunnel. This results in significant changes in amplitudes and arrival times both with and without the presence of the halo. The halo increases these effects, however. Additionally, the waveform character is altered at large offsets. Further details of the synthetic seismic results can be found in Bonal and Desilets (in progress).

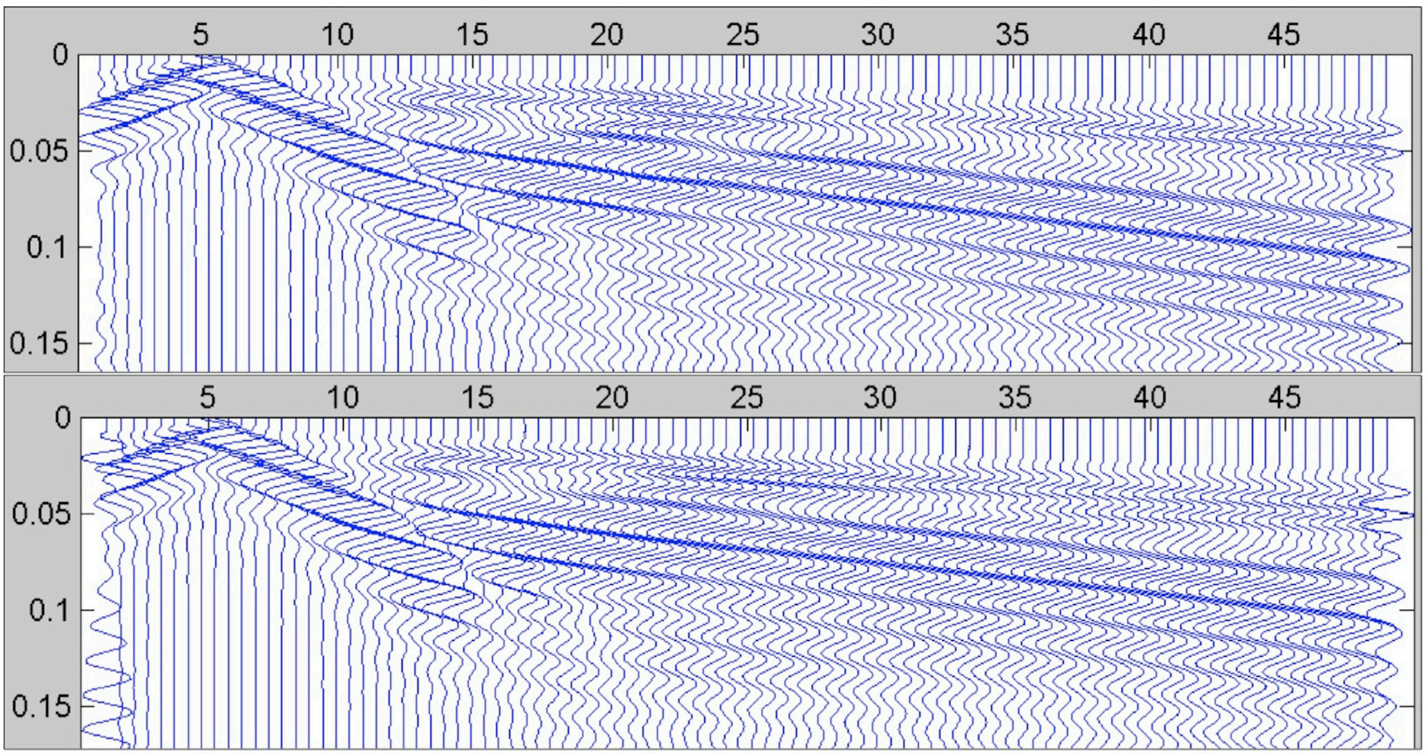


**Figure 3:** Examples of synthetic shot gathers for the model where the tunnel is located far above the water table. The x-axes are distance in meters and the y-axes are time in seconds. (Top) No tunnel is present in the model. (Bottom) Tunnel with halo is present in the model.

## Conclusions

Results show that the presence of a halo representing saturation, fracture, and stress changes decreases the impedance contrast between the air/rock interface. This decrease is not significant enough to completely mask the tunnel to seismic waves. In general, the hydrology response to a no-halo tunnel increases the spatial area of velocity disturbance by approximately an order of magnitude compared to the spatial area of the tunnel without considering changes in material properties surrounding the void. The effect of the halo region further increases the entire footprint. Furthermore, the halo area has a more significant impact on seismic waves than the void itself. So identifying changes in material properties rather than voids within the material may be a better way to locate cavities.

## Acknowledgements

Sandia National Laboratories is a multi-program laboratory managed and operated by Sandia Corporation, a wholly owned subsidiary of Lockheed Martin Corporation, for the U.S. Department of Energy's National Nuclear Security Administration under contract DE-AC04-94AL85000.

## References

Biot, M. A., 1956, Theory of propagation of elastic waves in a fluid saturated porous solid: I. Low-frequency range: Journal of the Acoustic Society of America, v. 28, p. 168–178.

Bonal, N. D. and Desilets, S. L. E., (in progress), Assessment of saturation changes around cavities and the impact on seismic waves.

Brutsaert, W., 1964, The propagation of elastic waves in unconsolidated unsaturated granular mediums: Journal of Geophysical Research, v. 69, p. 243–257.

Gardner, G. H. F., Gardner, L. W., and Gregory, A. R., 1974, Formation velocity and density - The diagnostic basics for stratigraphic traps: Geophysics, v. 39, p. 770–780.

Gassmann, F., 1951, Elastic waves through a packing of spheres: Geophysics, v. 16, no. 4, p. 673–685.

# INTERPRETATION OF SEISMIC TOMOGRAPHY RESULTS USING DATA QUALITY AND RESIDUAL ERROR MAPS

**Sonja Mackens, Geotomographie GmbH, Neuwied, Germany**
**Lutz Karl, Geotomographie GmbH, Neuwied, Germany**
**Thomas Fechner, Geotomographie GmbH, Neuwied, Germany**
**Daryl Tweeton, GeoTom LLC, Apple Valley, Minnesota**

**Corresponding Author:**
**Sonja Mackens, Geologist**
**Geotomographie GmbH**
**Am Tonnenberg 18**
**D-56567 Neuwied, Germany**
**email: smackens@geotomographie.de**

## Abstract

In seismic borehole tomography, the interpretation of the results is commonly limited to the comparison of the velocity map, the ray coverage, and the global root-mean-square RMS residual. However, the quality of the seismic data has a significant influence on the accuracy of the arrival time picking, but is generally not considered in the inversion. This paper presents an enhancement of the inversion taking into account the data quality, based on the signal-to-noise ratio, by using it to weight the traveltime residuals in each iteration step. This implementation also calculates the spatial distribution of the data quality and the distribution of the residual remaining at the end of the inversion, which are used to support the evaluation of a velocity map. The effect of the data weighting is studied on a field data set. Quality and residual maps are given and their relevance for the interpretation is discussed. The results indicate that areas of exceptionally high signal attenuation can be identified by means of the quality information.

## Introduction

Seismic borehole tomography is a well-established geophysical method providing high resolution information of the subsurface. Most commonly, the interpretation of the tomography results are limited to the evaluation of the seismic velocity map, the ray coverage, and the global RMS residual. The ray coverage is used to distinguish areas where the velocity map is trustworthy from zones of lower reliability. The global RMS is an important parameter for evaluating the general success of the inversion. Structural information about the subsurface are drawn from the seismic velocity map, which is the result of an inversion procedure using the first arrival times of the seismic signal.

***Keywords:*** Borehole Seismic Tomography, Simultaneous Iterative Reconstruction Technique (SIRT) Inversion, Traveltime Residuals.

It is well known that the data quality of seismic signals varies greatly, not only from region to region but even inside one data set. The data quality can vary from excellent (Figure 1) to very low (Figure 2). It is obvious that in the case of excellent data quality the first arrival time picking is easier and more accurate (Figure 1) compared to the picking of seismic signals which are contaminated by much noise (Figure 2). Generally, the data quality of seismic signals is not considered in the tomographic inversion. The present tomography inversion scheme mixes traveltimes of seismic signals with low and excellent data quality but treats them equally weighted within the inversion.

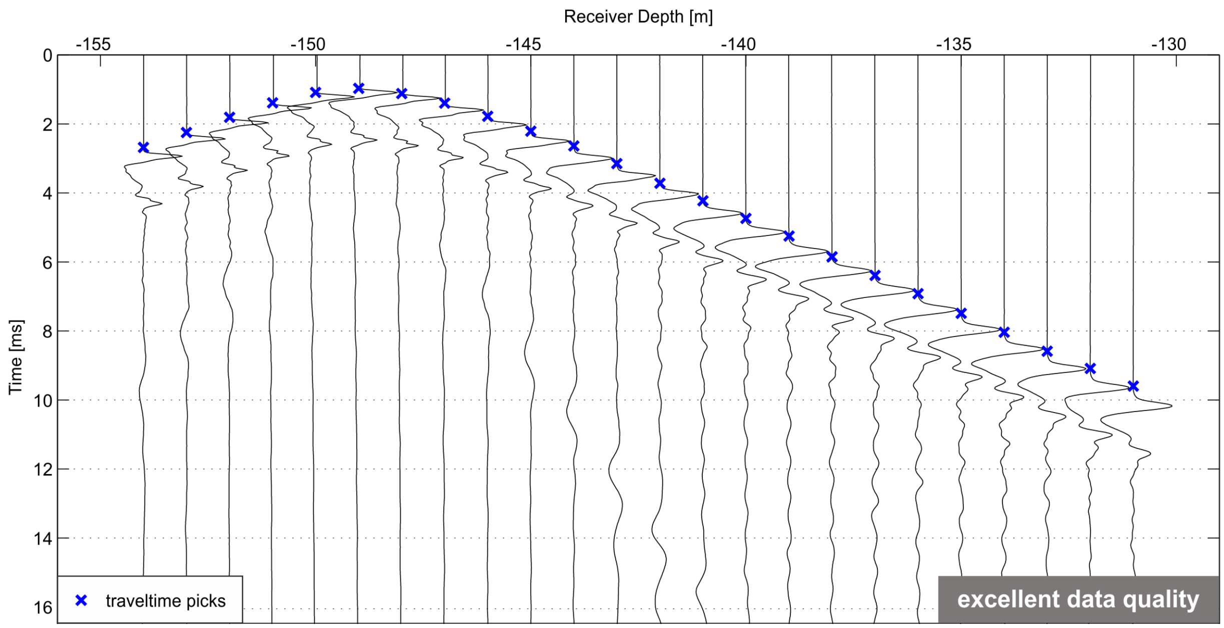


**Figure 1:** Seismic signals, gathered in saturated sand, showing excellent data quality.

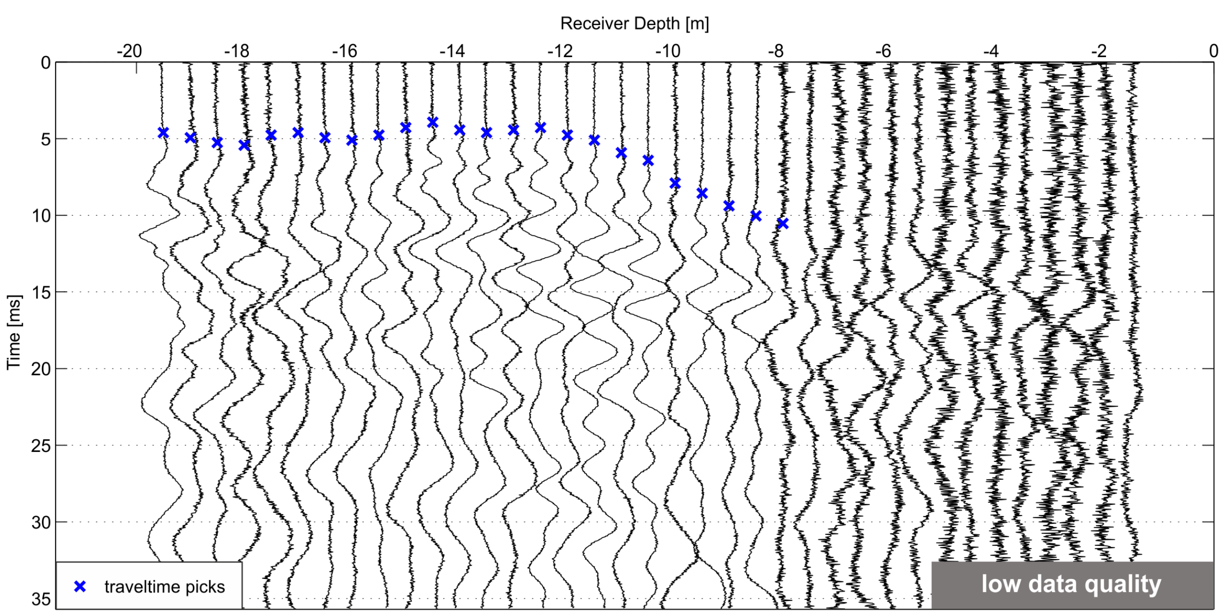


**Figure 2:** Seismic signals, gathered in weathered unsaturated limestone, showing low data quality.

This paper presents an enhancement of the inversion taking into account the data quality, based on the signal-to-noise ratio, by using it to weight the traveltime residuals in each iteration step. Furthermore, the implementation calculates the spatial distribution of the data quality and the distribution of the traveltime residual remaining at the end of the inversion. These two additional values are used to support the evaluation of a seismic tomography velocity map.

## Data Quality Weighting

It is obvious that the signal-to-noise ratio influences the accuracy of a traveltime pick. Thus, the larger the noise, the lower the reliability of a traveltime pick. If the related uncertainty is not addressed within a tomographic inversion process, all picked traveltimes have the same weight and contribute equally to the determination of the seismic velocities within a seismic tomogram. In other words, a seismic velocity determined by a "perfect" traveltime pick competes with an uncertain velocity estimate of a poor traveltime pick. Therefore, equally weighted traveltimes are not the best assumption, as seismic field data are often contaminated by noise of different amplitude and the data quality ranges from perfect quality to useless.

Ray coverage as a measure of ray density per volume is a common criterion to decide if a seismic velocity and the related velocity structure are trustworthy. Lehmann (2007), describes those and other factors affecting quality, resolution, and uncertainty. Guiding the tomographic Simultaneous Iterative Reconstruction Technique (SIRT) inversion of seismic traveltime data with respect to geometrical weighting factors is described by several authors (Krajewski, and others, 1989; Lehmann, 1992; Tinti and Ugolini, 1990). For instance, such weighting schemes take the different geometrical ray density or the ray azimuth into account, i.e., less weight will be applied to areas of lower ray density or to those areas with less azimuthal coverage. However, the weighting is only related to geometrical parameters and does not consider the data quality itself.

To evaluate directly the dependency between signal-to-noise ratio and traveltime picking accuracy, we performed a statistical analysis by generating synthetic wavelets. The signal-to-noise ratio is calculated by the ratio of the maximum first arrival amplitude and the average noise amplitude before the first arrival. This factor is called quality factor (QF) within our numerical implementation. QF values are normalized to the highest QF value in a data set. An example plot of the synthetic seismic signals is shown in Figure 3.

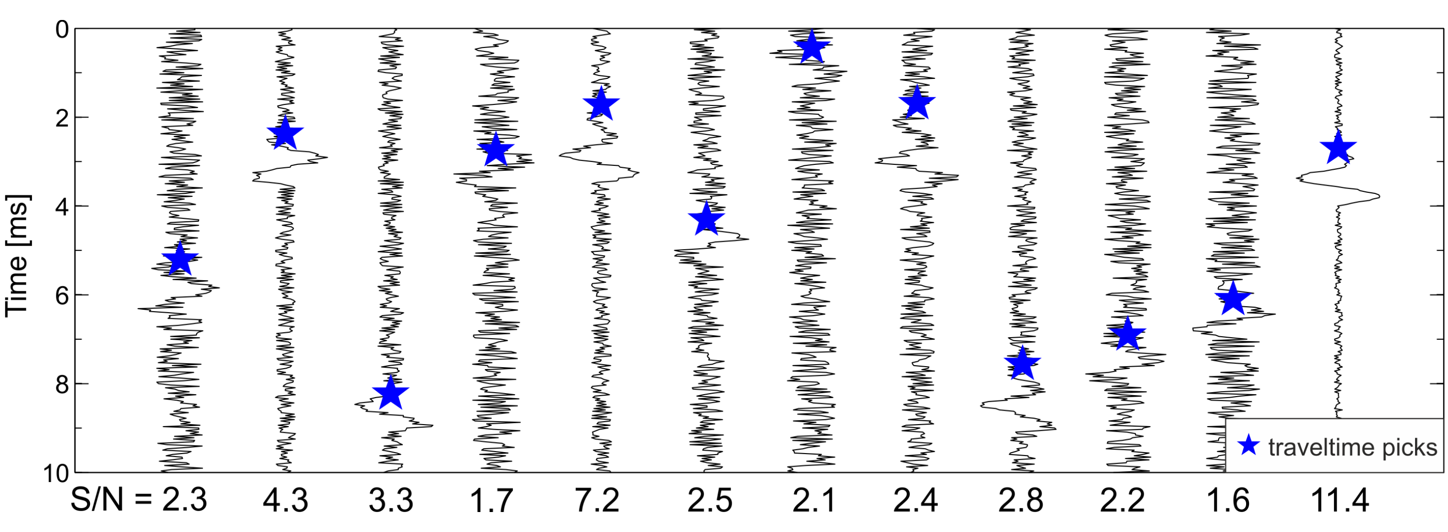


**Figure 3:** Synthetic seismic signals showing different signal-to-noise ratios and picked traveltimes (blue stars).

First arrival times were picked from modelled seismic signals to allow a basic statistical analysis. Traveltime errors were plotted versus the signal-to-noise ratio and an appropriate trend line was fitted to the mean traveltime picking errors as well as to the standard deviations of the traveltime picks. The results of the analysis are shown in Figures 4 and 5. The plots show how the average traveltime picking error and the standard deviation of the picking error decrease with increasing signal strength.

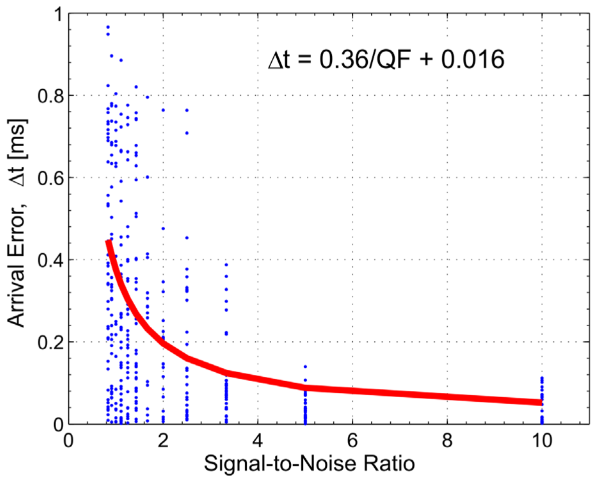


**Figure 4:** Average picking error.

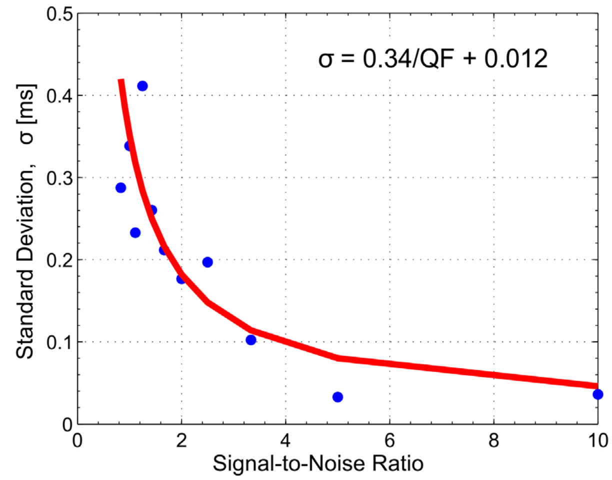


**Figure 5:** Standard deviation of picking error.

The plots show further that the improvement in accuracy of picking times tends to level off as the signal-to-noise ratio continues to improve, so the QF values assigned to represent data quality should reach a maximum at some threshold instead of continuing to increase with increasing signal-to-noise ratio. To account for the traveltime picking error, we introduce a data quality dependent weighting into the well-known SIRT tomography inversion procedure. Within this procedure, we assign a QF value to each seismic ray "k" calculated from the signal-to-noise ratio of the seismic trace. The QF value (normalized signal-to-noise ratio) is implemented in the SIRT slowness correction scheme (see Equation 1):

$$\Delta s_n = \frac{1}{\sum_k QF_k} \cdot \sum_k \frac{QF_k \cdot \Delta t_k \cdot r_{n,k}}{\sum_m r_{m,k}^2} \quad (1)$$

where

$\Delta t_k$ is the traveltime residual of ray "k",
$r_{n,k}$ is the length of the raypath segment (ray "k") in voxel "n",
m is the index of raypath segments belonging to ray "k",
$QF_k$ is the quality factor of ray "k", and
$\Delta s_n$ is the slowness residual in voxel "n".

If all QF values are equal, equation 1 reduces to the SIRT slowness correction scheme. The implementation of the QF value in the inversion procedure will give higher weight to rays with higher QF value. As a consequence, seismic velocities of rays with higher QF will be have greater influence in a cell than those with lower QF, i.e., the averaged velocity comes closer to the seismic velocity of higher weighted rays. After the final iteration, the distribution of the average QF value in each cell or voxel can be plotted next to the seismic velocity distribution. The QF value distribution shows areas with low and high QF value, thus with lower or higher reliability of the seismic velocity. In this way, the QF value distribution supports the interpretation and evaluation of a seismic tomogram. An example is shown in Figure 6.

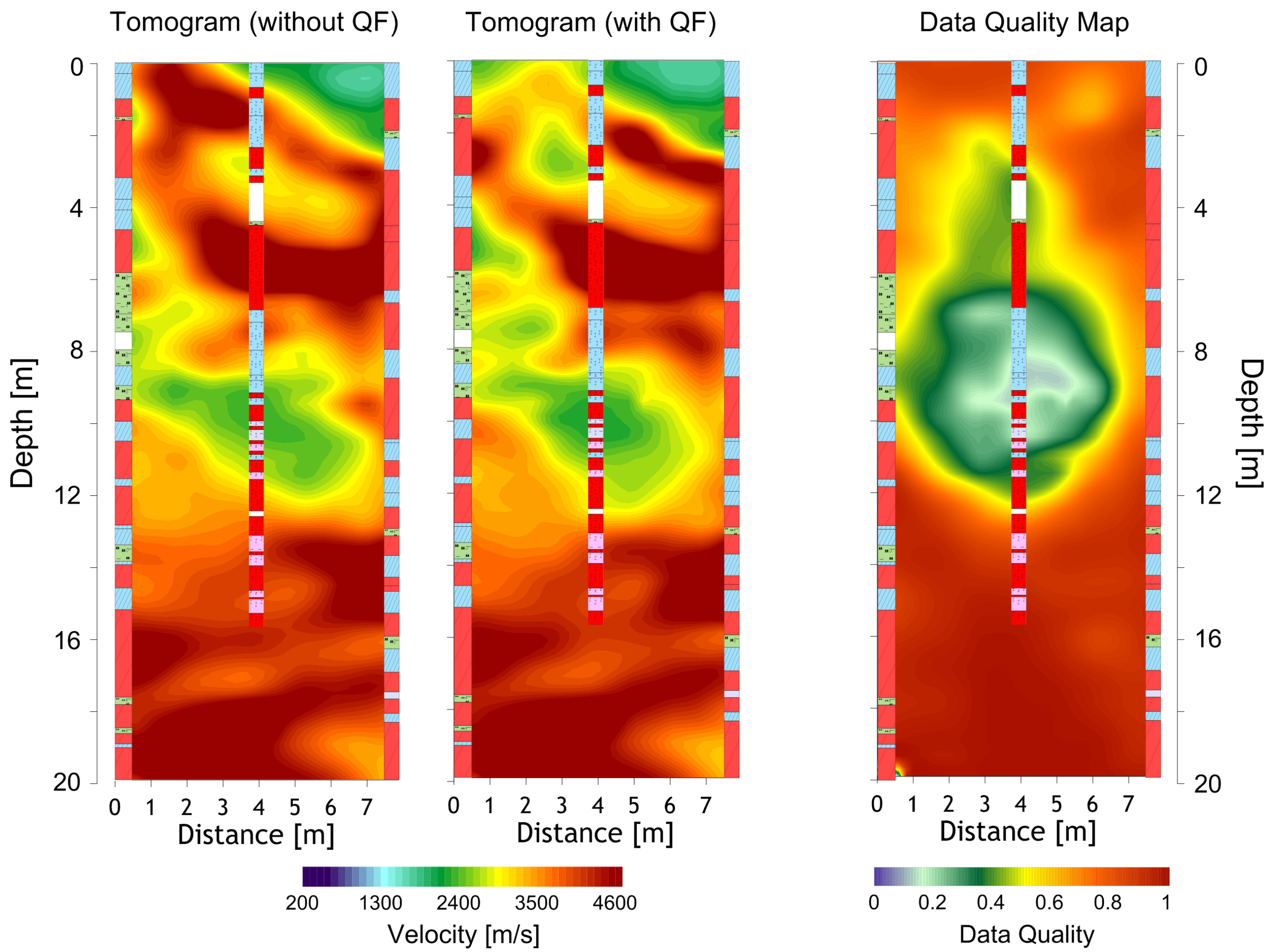


**Figure 6:** Seismic tomogram without QF (left), seismic tomogram with QF (middle) and related QF value map (right). Coring information is displayed for three boreholes (red – hard rock, blue – weathered rock, green – soft rock, white – cavity).

In general, the seismic tomograms displayed in Figure 6 do not show large differences. The main zonation, such as the high and low velocity areas at the top, the middle and the bottom of the tomograms is similar, as is as the velocity range. However, there are small changes visible in the tomogram inverted using the QF values leading to better differentiation, i.e., less smooth structures. For example, the center area with lower seismic velocities shows a higher resolution especially between the left and middle boreholes. Furthermore, the area around the cavity found at 4 m depth in the middle borehole is sharpened and shows a better resolution. The distribution of the QF values is shown on the right side of Figure 6. Areas with low QF values are in general areas where the velocity determination is less reliable, whereas higher QF values point to a more reliable velocity estimate. Low QF values may correspond to material with higher absorption. Within the QF value distribution, a large area with low QF values is shown in the center part, pointing to material with higher absorption than in other areas. Moreover, the area around the cavity in the middle borehole also shows very low QF values, supporting the seismic tomogram interpretation of the existing cavity. Material of excellent rock quality shows typically higher QF values. This pattern is in agreement with the coring information, especially for the section below 12 m. Thus, we conclude that the implementation of the QF values for seismic inversions offers additional and valuable information for the interpretation of a seismic tomogram.

## Residual Error Maps

Iteration progress is measured by the RMS value of the seismic traveltime residual, i.e., measured minus calculated traveltime. The RMS value in most cases remains non-zero, pointing to a non-perfect fit. The small misfit of each traveltime residual can be transformed into a slowness error per voxel. One calculates the slowness residual for each voxel as in Equation 1 and divides it by the slowness in that voxel calculated during the final iteration. One then obtains a relative slowness residual error, as displayed in Figure 7. Areas with relative slowness residual errors close to 0 indicate good estimates of the local seismic velocity. Negative or positive relative slowness residual errors are a sign of underestimated or overestimated velocities, respectively.

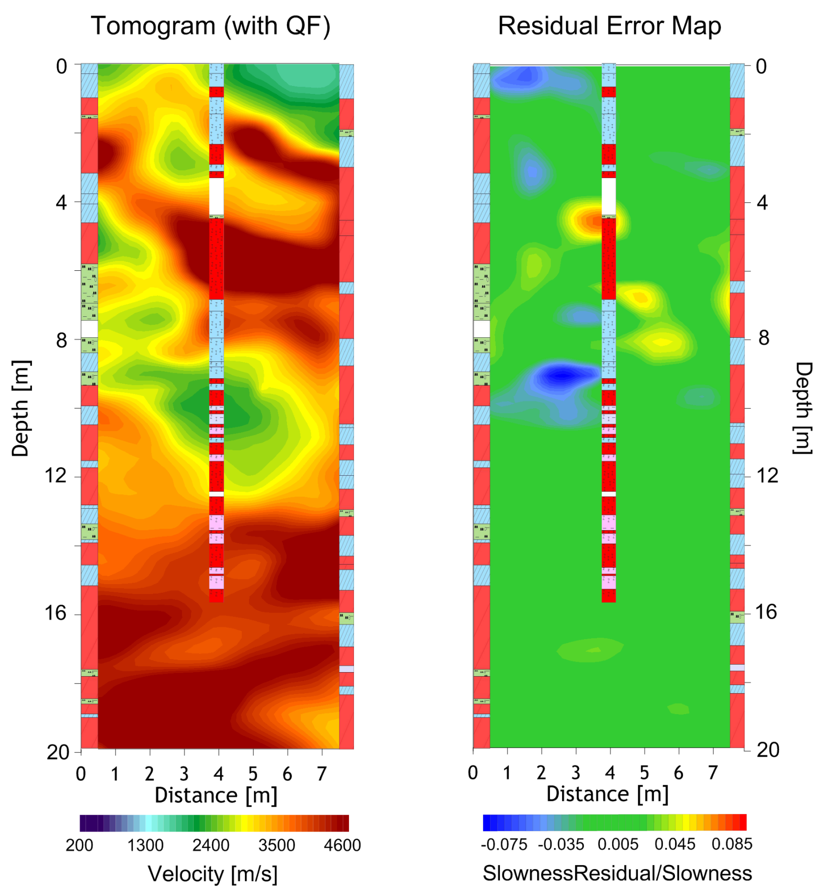


**Figure 7:** Seismic tomogram with QF (left) and residual error map (right).

## Implementation

The procedure has been implemented in GeoTom software. The time-picking software TomTime calculates data quality factors from signal-to-noise ratios. The tomographic inversion software GeoTomCG allows those and other data quality factors to be part of the input data. Thus, the data quality factors can be based entirely on the signal-to-noise ratio or can also take into account other factors judged to affect reliability.

## Conclusions

A new data quality weighted seismic traveltime inversion scheme has been presented. The weighting scheme was implemented into the well-known SIRT procedure. Data quality was calculated based on the signal-to-noise ratio of the seismic data. In principle, the data quality weighting allows any individual data quality criteria to influence the inversion procedure. The data quality weighting allows the reliability of the resulting seismic tomogram to be interpreted in terms of the chosen quality criteria. In addition, a procedure to access remaining relative slowness errors after the final iteration is described. The data quality weighted inversion has been successfully tested on field data.

## Acknowledgments

We thank Wendy Albers and Markus Kunert for their contribution to the improvement and testing of the data quality weighted traveltime tomography.

## References

Krajewski, C., Dresen, L., Gelbke, Ch., and Rueter, H., 1989, Iterative Tomographic Methods to Locate Seismic Low-Velocity Anomalies: A Model Study, Geophysical Prospecting 37, Issue 7, P. 717-751.

Lehmann, B., 1992, Modellseismische Untersuchungen zur Transmissions- und Reflexionstomographie unter Verwendung der Gauß-Beam Methode, Phd-Thesis, Ruhr-University Bochum, Reihe A, Nr. 33 (in German).

Lehmann, B., 2007, Seismic Traveltime Tomography for Engineering and Exploration Applications, EAGE publications bv, DB Houten, The Netherlands, P. 37-57.

Tinti, S. and Ugolini, S., 1990, Pre-Selection of Seismic Rays As a Possible Method to Improve the Inverse Problem Solution, Geophysical Journal International 102, Issue 1, P. 45-61.

# APPLICATION OF SHALLOW SEISMIC REFRACTION FOR DETERMINING GEOTECHNICAL PROPERTIES AND COMPETENCE OF KARSTIC LIMESTONE BEDROCK IN AN AREA WEST OF ASSIUT, EGYPT

**Ali H. Abdel Aati, Professor (Corresponding Author)**
**Geology Department**
**Faculty of Science**
**Assiut University**
**71516 Assiut, Egypt**
**email: ahaati@yahoo.com**

**Sabah H. Shabaan, Senior Geophysicist**
**General Petroleum Company**
**8 Dr. Mostafa Abu Zahra St., Nasr City**
**Cairo, Egypt**
**email: sabah.hamed@yahoo.com**

## Abstract

The main objective of this study was to determine the geotechnical properties of subsurface karstic limestone bedrock on the lower Eocene plateau, west of Assiut, Egypt. A shallow seismic refraction survey was conducted along eight profiles in different directions using a 12-channel exploration seismograph (Geometrics Model 1225 ). The P-wave seismic velocities were recorded using in-line spread and vertical geophones while the S-wave seismic velocities were recorded using horizontal geophones. The seismic refraction technique is considered a powerful tool for computing the kinetic elastic moduli and other geotechnical properties, which give important information about the degree of consolidation and the material competence of foundations. These geotechnical properties for foundation bedrock were calculated and presented in contour maps. The presence or absence of competent and high quality material at the foundation location define its suitability for constructing buildings and civil engineering projects. It was found that the P-wave seismic velocities range from 2800 to 4500 m/s and the S-wave seismic velocities range from 1600 to 2750 m/s. It was also concluded that the values of elastic moduli measured in the petrophysical laboratory are consistent with the results obtained from the field . Also, the computed geotechnical properties within the bedrock have been used for dividing the study area into three zones of different rock competence.

***Keywords:*** Seismic Refraction, Geotechnical Properties, Karstic Limestone Bedrock.

## Introduction

Urban expansion and the establishment of new cities and communities in the Western Desert near Assiut, Egypt are needed to solve population density problems. Shallow seismic refraction techniques has been important for use in determining rock quality and the best sites for civil engineering projects. The value of this geophysical method is not only for determining layer velocities and thicknesses, but also for defining depth to bedrock, its competence, and other geotechnical properties. Geotechnical properties are very important in solving practical engineering problems of foundation design as well as giving information about the physical characteristics of foundation materials. The main objective of this study was to use seismic refraction methods to evaluate geotechnical properties, especially the competence, of the karstic limestone bedrock. The integrated analysis of both compressional and shear waves is necessary for calculation of the geotechnical properties and competence of the foundation layer. Also, suitability of the bedrock for construction of buildings and other civil engineering projects can be evaluated. The shear wave velocity is much more sensitive to changes in lithology and geotechnical properties than the compressional wave velocity, which is characterized by a narrow range of values. Therefore, shear wave surveys appear to be more suitable for engineering site investigations than compressional wave surveys. Generally, the shallow seismic refraction technique is a powerful tool for computing the kinetic elastic moduli and other geotechnical properties, which give some information about the degree of consolidation and the material competence of the foundation rock layer. The kinetic elastic moduli as well as the other geotechnical properties of the foundation layer were calculated and presented in the form of contour maps. With no previous shallow geophysical work in the area, this study provided essential baseline characteristics for evaluating and developing urban settings.

## Geologic Setting

The study area measures approximately 3 $km^2$ (Figure 1). The area is topographically flat and its elevation is nearly 222 m above sea level. It lies on a Lower Eocene limestone plateau west of Assiut. The exposed Lower Eocene deposits near Assiut are divided into three rock formations from base to top as follows (Figure 2) (Omara et al.,1970);

1) Zawia Formation,
2) Drunka Formation, and
3) Matmar Formation.

The study area site is considered the best location for urban expansion and construction of new suburbs and communities (Abdel Aati, 1995 and Abdel Aati and Shabaan, 2013). The limestone bedrock belongs to the Drunka Formation (Figure 2). This limestone is characterized by distinctive layering, local reef or lagoonal depositional environments, with concretions, local flint bands, and cherty nodules. The Drunka Formation is expansive and covers a wide area. It represents the main part of the Lower Eocene limestone plateau and is currently quarried for building materials. The soil is composed of gravel and silt. Hard massive limestone is exposed at the surface in certain locations. Some clear karstification of the limestone is exposed in an outcrop near the study area (Figure 3) (Waltham, 1994).

Relatively little information about the subsurface geology in the study area is known. No wells have been drilled in this area. Prior to this study, the only documented near-surface geologic information for this area was inferred from a lithological cross section produced from surficial mapping of a wall exposed in an excavation trench. Three distinct layers clearly exposed in the trench wall include top soil, weathered limestone, and the hard limestone bedrock (Figure 4) (Shabaan, 2008).

**Figure 1:** The naturally flat and extensive study area belonging to Drunka Formation.

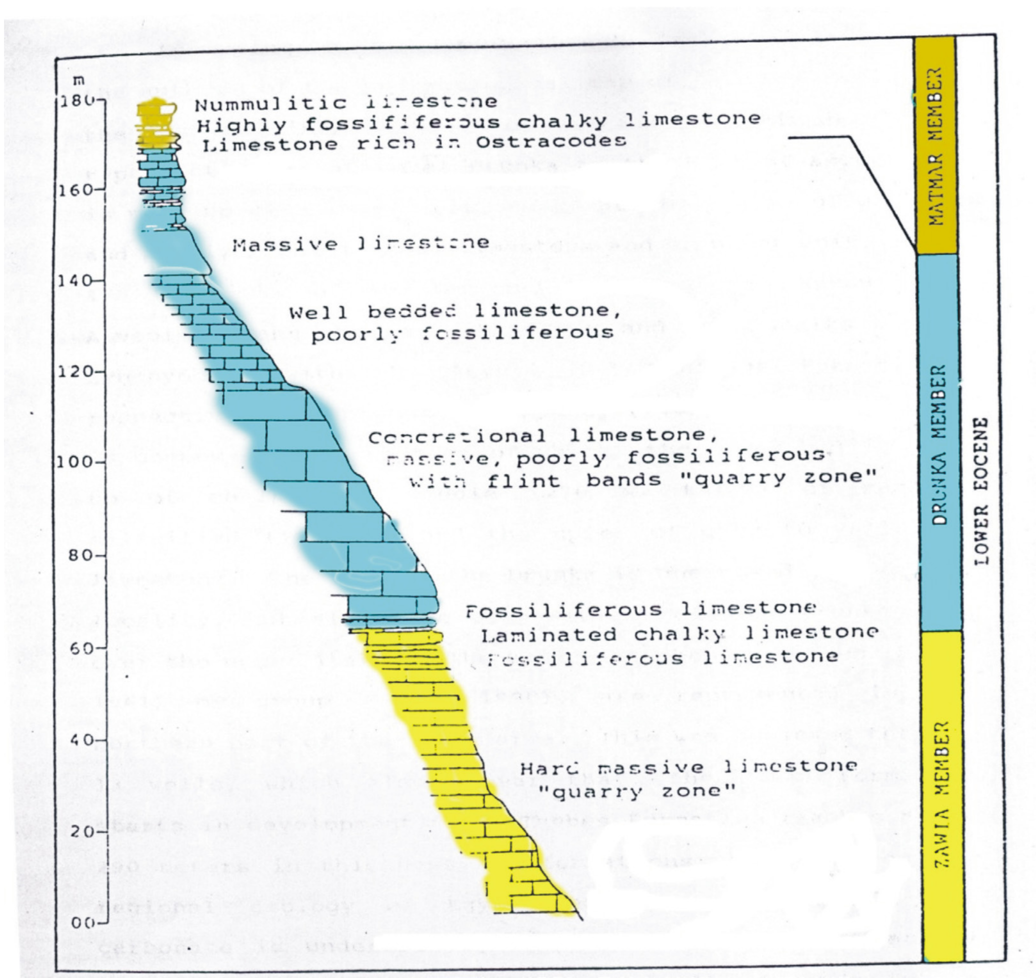


**Figure 2:** Stratigraphic cross section in the western scarp of Drunka village (Omara et al., 1970).

**Figure 3:** Clear karstification exposed on the scarp near the study area (Youssef et al., 2003).

**Figure 4:** Lithological cross section inferred from artificial excavation around the area.

## Fieldwork

A shallow seismic refraction survey was conducted along eight profiles in the study area using a 12-channel exploration seismograph (Geometrics Model 1225). Five of these profiles were oriented east-west and the other three profiles were aligned north-south (Figure 5). The main goal of these seismic geophysics field measurements was to evaluate the P-wave and S-wave velocities, and in turn, geotechnical properties, such as the kinetic elastic moduli of the foundation bedrock. This information provides the degree of consolidation, the material competence, and the quality of the rock mass, which defines the suitability of the foundation bedrock for construction of buildings and other civil engineering projects.

For this study, the survey design called for 170 shot points to be distributed along continuous seismic profiles with both normal and reverse shot directions. Each spread is 120 m with eight spreads grouped to make each of the five east-west lines. Each of the three north-south profiles is approximately 1.5 km in length and is composed of approximately 11 spreads. For optimally capturing these P-wave first arrivals, vertical geophones, each separated by 10 m, were used.

P-wave seismic records obtained in proximity to the trench face (forward and reverse) possessed interpretable, strong first arrivals with timing accuracy in the sample range (Figure 6). The time-distance graphs exhibited good quality. Example time-distance curves and associated geoseismic cross section (Figure 7) are from near the excavation cut wall. Correlating the cross section with the geology exposed in the cut face provided an excellent opportunity to ground truth the accuracy of the velocity-depth cross section.

For optimally capturing the S-wave first arrivals, horizontal geophones each separated by 5 m were used. Three spreads were carried out along each of the east-west profiles to measure velocities of S-waves. Example S-wave seismic records obtained from Spread A along Profile 2 (forward and reverse) are evident in Figure 8.

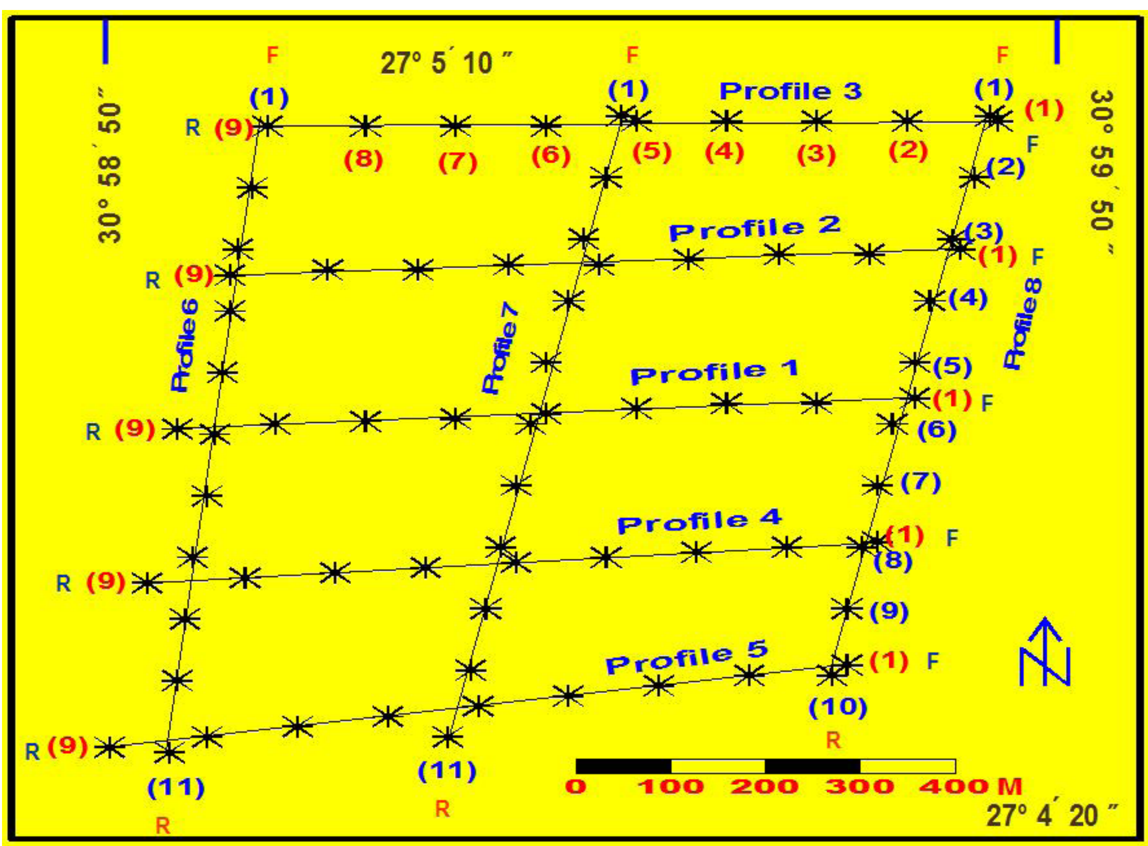


**Figure 5:** Location map of seismic profiles and shot points in study area.

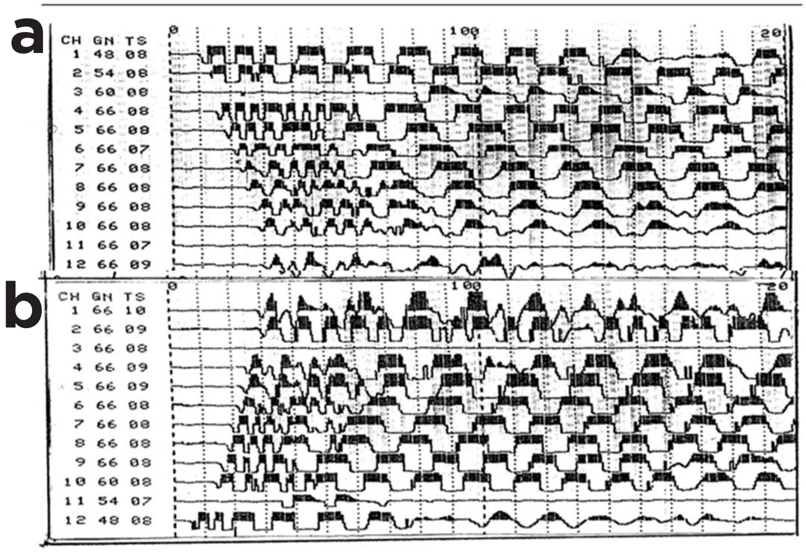


**Figure 6:** Examples of P-wave seismic records along artificial excavation Profile AP4M: (**a**) forward and (**b**) reverse.

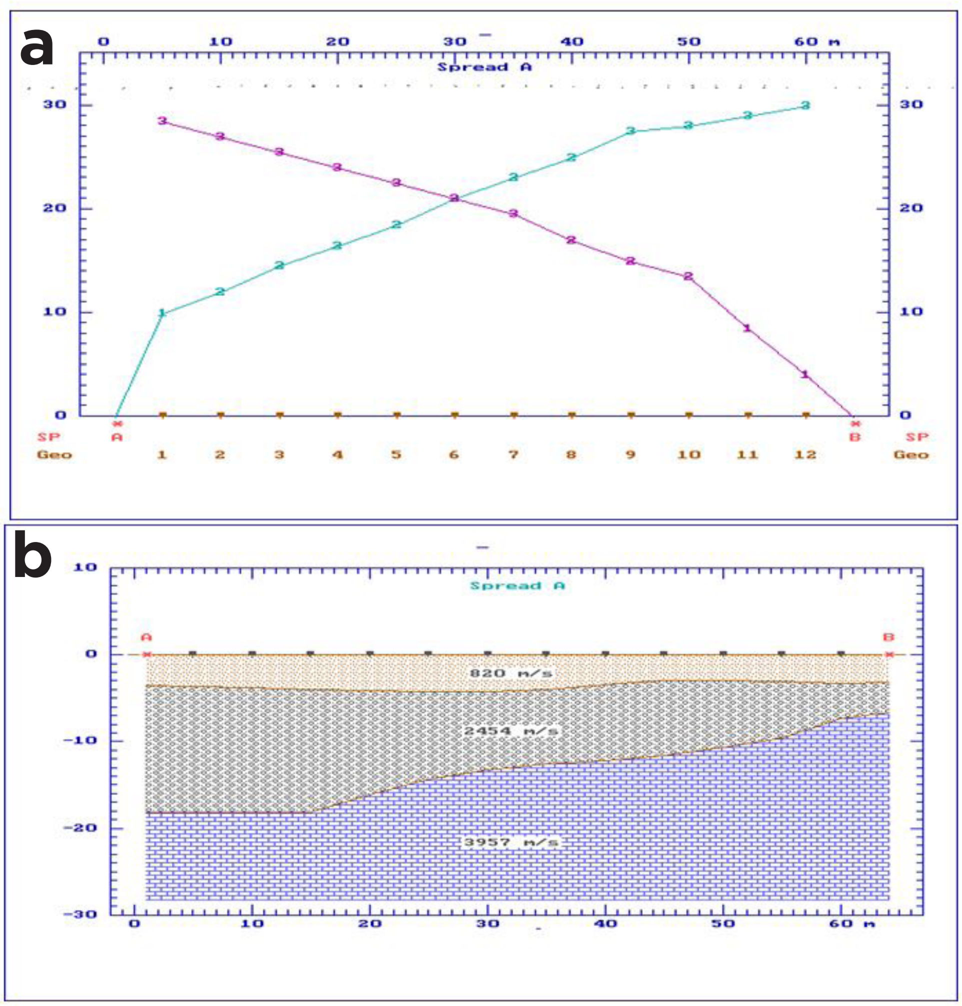


**Figure 7:** (**a**)Time-distance graph along artificial excavation profile (AP4M) for P-waves and (**b**) geoseismic cross section along artificial excavation profile for P-waves

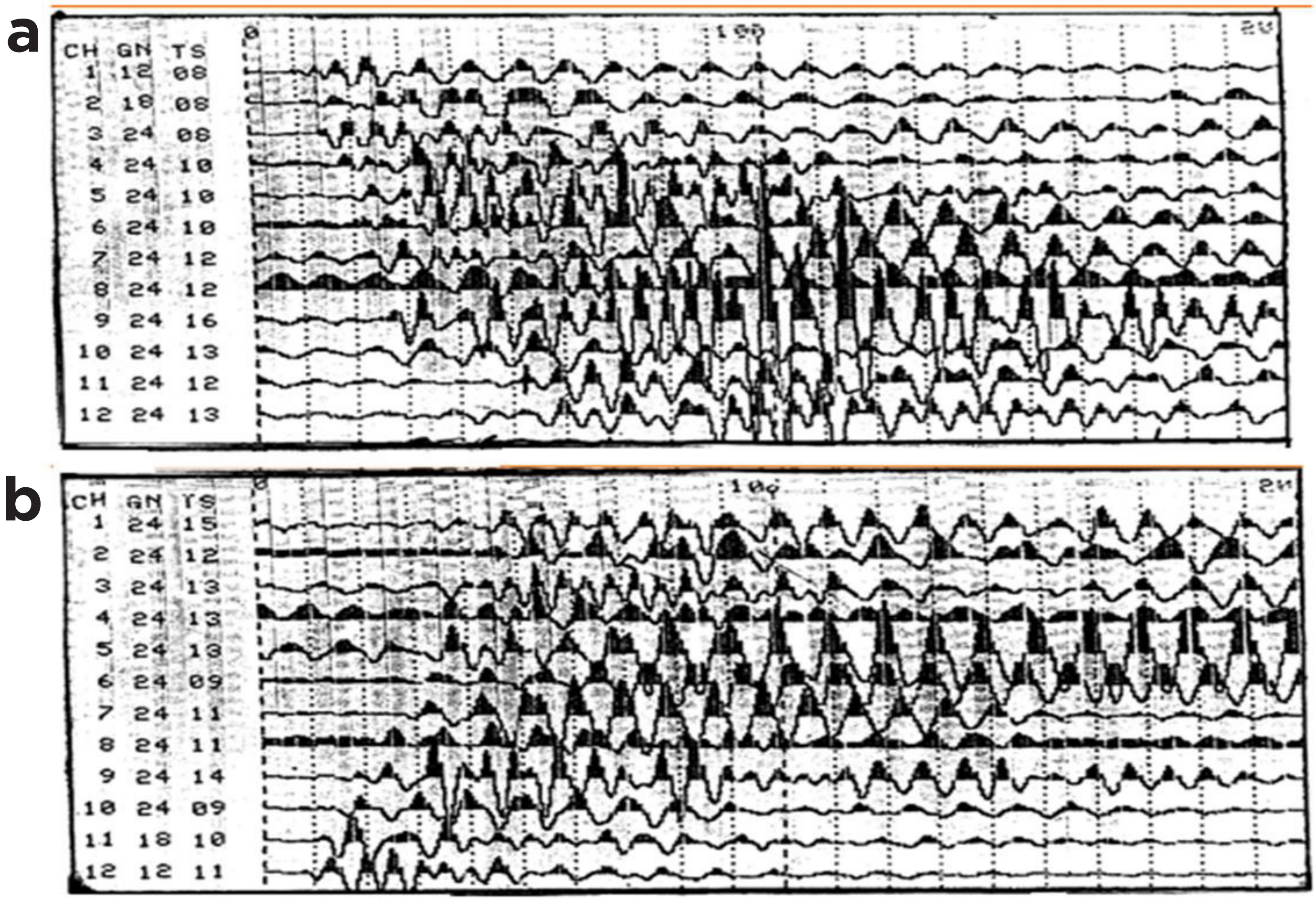


**Figure 8:** Examples of S-wave seismic records of Spread A along Profile P2AS; (**a**) forward and (**b**) reverse.

## Evaluation of Foundation Bedrock Geotechnical Properties

The interpretation process started with manual graphical estimation of the number of layers for each spread and their associated seismic velocities. Before evaluation of geotechnical properties, P-wave and S-wave velocity contour maps were constructed to provide a high-resolution maps indicative of rock strength and anomalous footing areas. Data were interpreted using the SIP software program (Rimrock Geophysics, 1997) which allowed the calculation of the geoseismic cross section for each spread. The P-wave velocities ($V_P$) of the bedrock limestone range from 2800 to 4500 m/s (Figure 9) while the S-wave velocities ($V_S$) of the same foundation bedrock range from 1600 to 2750 m/s (Figure 10).

From the integration analysis of P- and S-wave velocities, the geotechnical properties of the foundation bedrock were computed and presented in contour maps for the whole study area. The geotechnical properties were classified into three categories as follows:

1) kinetic elastic moduli including Poisson's ratio (σ), $V_P/V_S$ ratio, Young's modulus (E), rigidity (shear) modulus (μ), and bulk modulus (k);

2) rock material competence values including material index ($M_i$), concentration index ($C_i$), stress ratio ($S_i$) and the A-value; and

3) foundation material bearing capacities including ultimate bearing capacity ($Q_{ult}$) and allowable bearing capacity ($Q_a$).

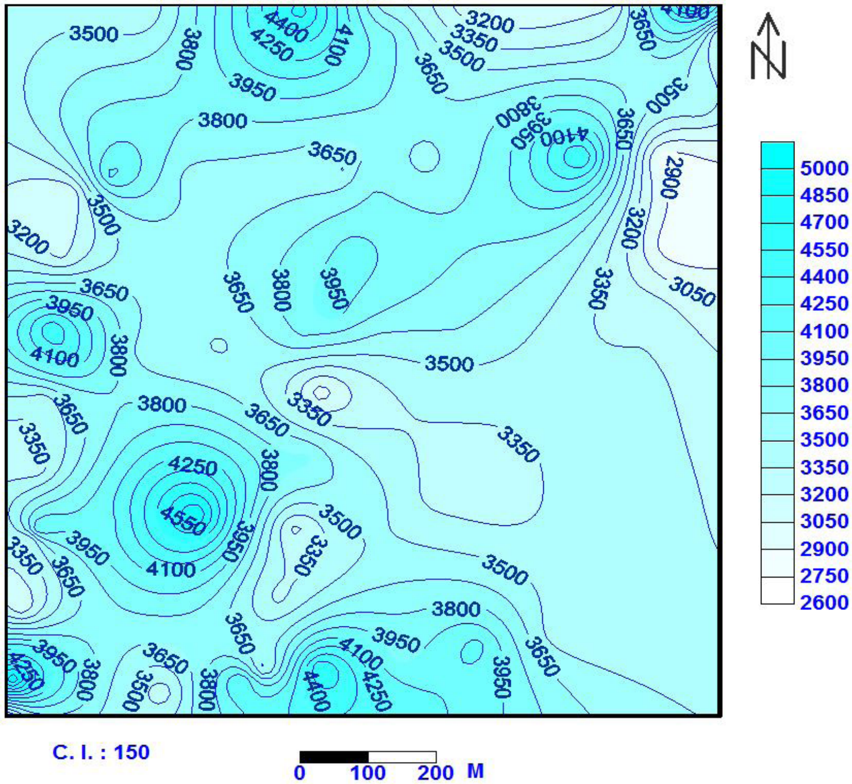


**Figure 9.** Distribution of the P-wave compressional velocity in m/s ($V_P$) for the foundation bedrock layer.

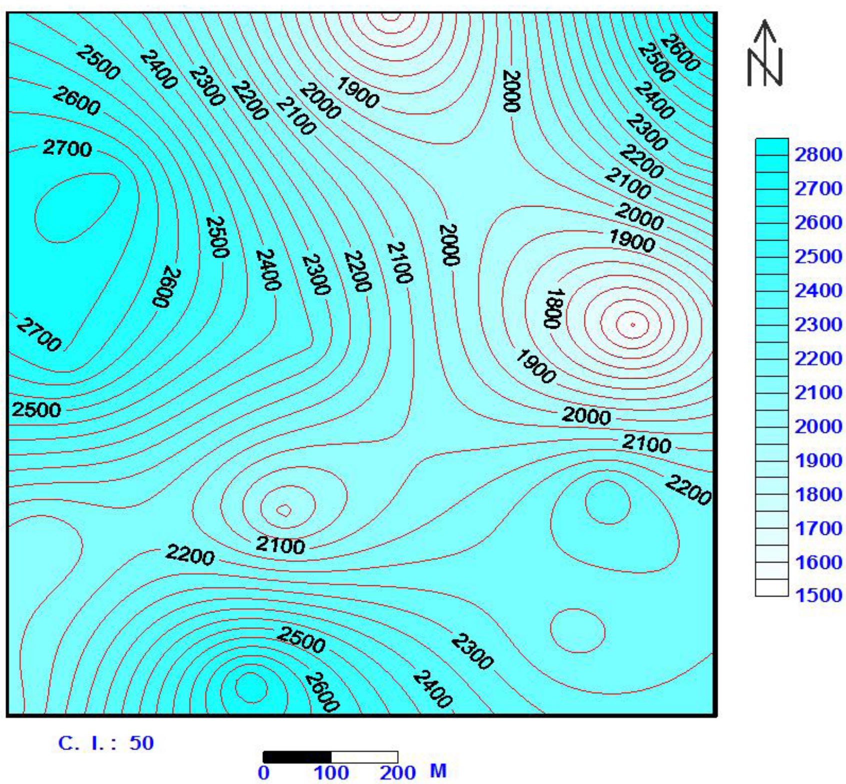


**Figure 10.** Distribution of the S-wave shear velocity in m/s ($V_s$) for the foundation bedrock layer .

**Kinetic Elastic Moduli of Rock Material**

***Poisson's Ratio (σ)*** - Poisson's ratio is defined as the ratio of transverse strain to longitudinal strain. It can be calculated using P- and S-waves velocities by the equation:

$$\sigma = 1 - 2(V_S^2/V_P^2)/2(1-V_S^2/V_P^2) \quad . \qquad (1)$$

Higher values of σ indicate weak, incompetent materials, while lower values indicate strong, competent material. Negative values represent very competent, indurated materials. Figure 11 shows the distribution of Poisson's ratio in the foundation layer.

***$V_P/V_S$ Ratio*** - The $V_P/V_S$ ratio can be calculated using σ as follows:

$$V_P/V_S = ((1-\sigma)/(0.5-\sigma))^{0.5} \quad . \qquad (2)$$

According to the data (Packett, 1963 ), which yields a $V_P/V_S$ value about 1.9 for limestone. Lower values of the $V_P/V_S$ ratio indicate higher material quality. Figure 12 shows the distribution of $V_P/V_S$ in the foundation bedrock.

***Young's Modulus (E)*** - Young's modulus is defined as the stress/strain ratio when the body is pulled or compressed. It can be expressed in terms of rigidity modulus (μ) and Poisson's ratio (Imai, 1975) by the equation:

$$E = 2\mu(1 + \sigma) \quad . \qquad (3)$$

Larger values of Young's modulus indicate higher material quality and stiff rocks. Figure 13 shows the distribution of Young's modulus in the bedrock.

***Rigidity (Shear) Modulus (μ)*** - The rigidity modulus represents resistance to shear stress or dynamic rigidity. It is a measure of the stress/strain ratio in the case of a simple tangential stress (Sharma, 1976). The rigidity modulus can is defined by the following equation:

$$\mu = \rho_b V_S^2 \quad , \qquad (4)$$

where $\rho_b$ is the bulk density. The bulk density of the rock materials can be calculated using the compressional wave velocity as follows:

$$\rho_b = 1.62 + 0.00021V_P \quad . \qquad (5)$$

Low values of rigidity modulus (μ) indicate low competent and low rigid materials, while higher values of μ indicate competent rocks. Figure 14 shows the distribution of rigidity in the bedrock.

***Bulk Modulus (k)*** - Bulk modulus (k) is the measure of volumetric change due to volumetric force. The bulk modulus is given by the following equation:

$$k = E/(3(1 - 2\sigma)) \quad . \qquad (6)$$

Bulk modulus increases with an increase of Poisson's ratio. Also, higher values of bulk modulus indicate lower material quality. Figure 15 shows the distribution of the bulk modulus in the bedrock.

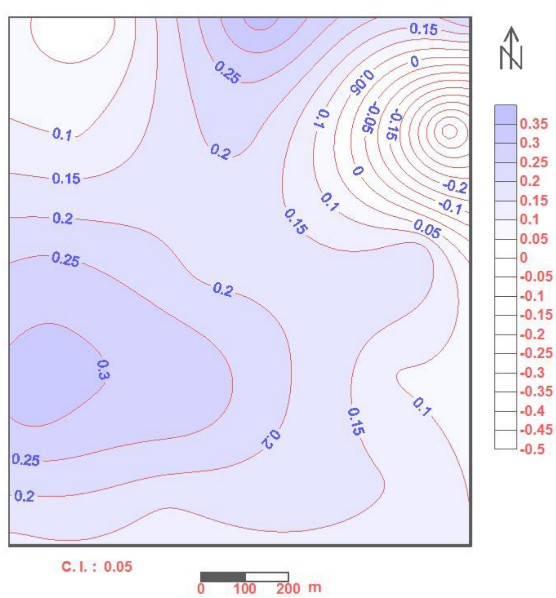


**Figure 11:** Distribution of poisson's ratio (σ) for the foundation limestone bedrock layer.

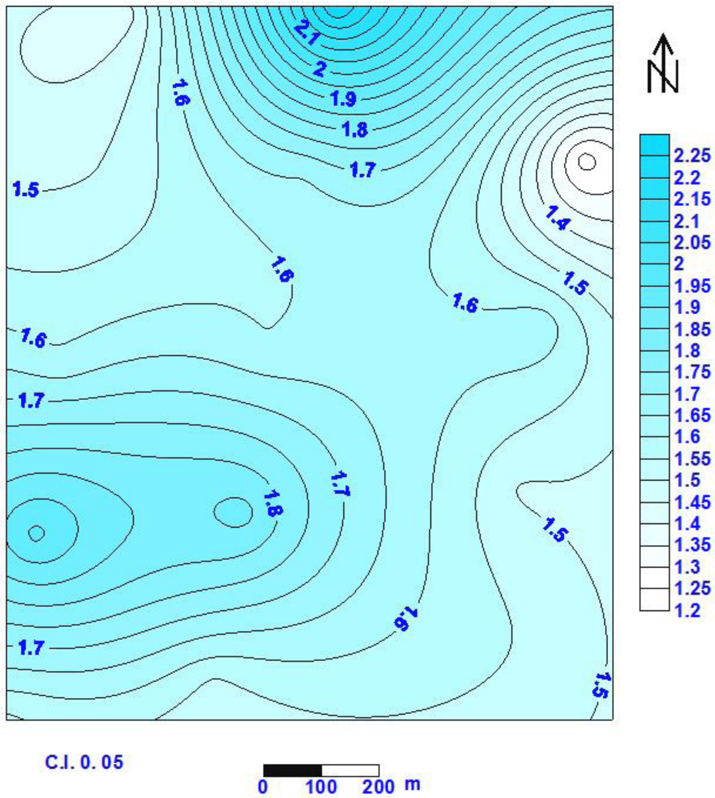


**Figure 12:** Distribution of $V_P/V_S$ ratio for the foundation bedrock layer.

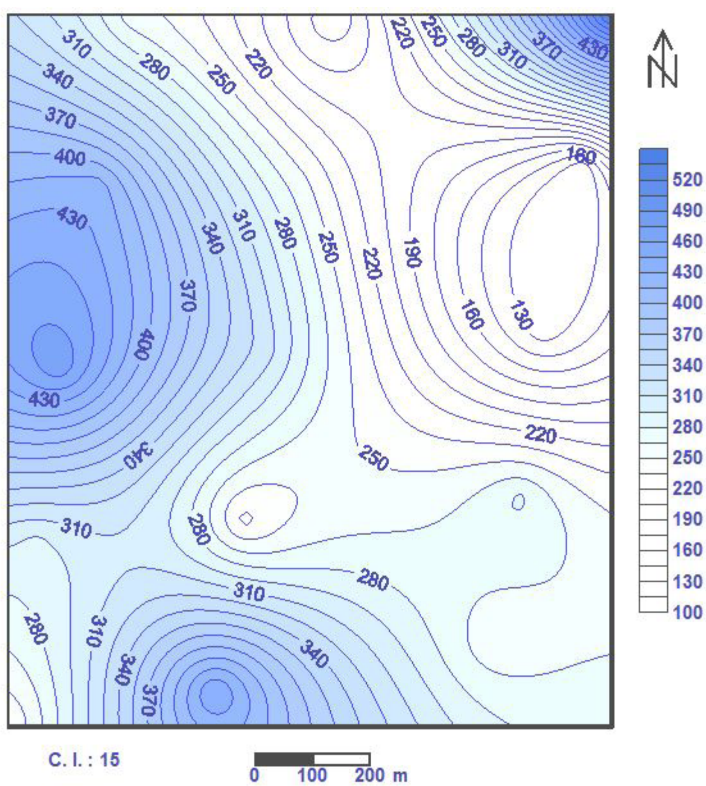


**Figure 13:** Distribution of Young's modulus (E) in g/cm$^2$ for the foundation bedrock layer.

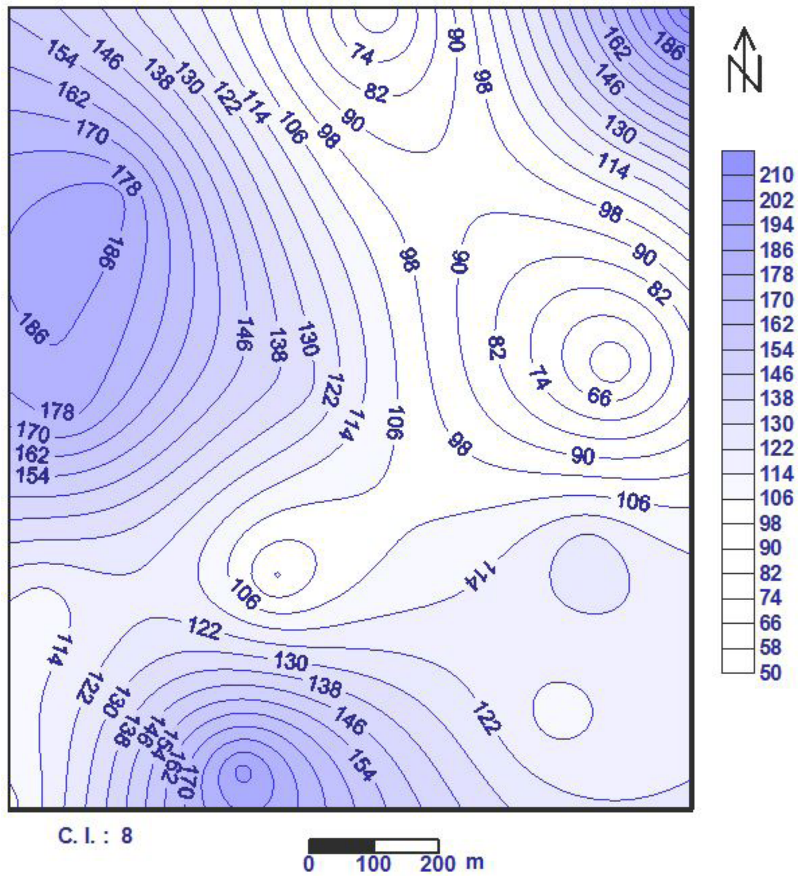


**Figure 14:** Distribution of rigidity modulus (μ) in g/cm² for the foundation bedrock layer.

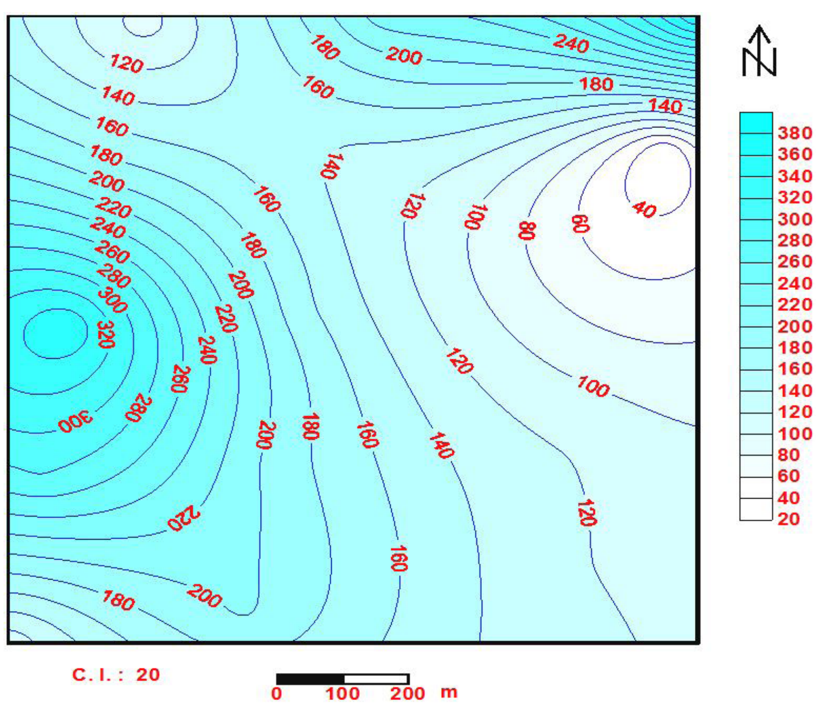


**Figure 15:** Distribution of bulk modulus (k) in g/cm² for the foundation bedrock layer.

**Rock Material Competence Values**

***Material Index ($M_i$)*** - The material index is defined as the degree of competence for a material based on kinetic elastic moduli (Abdel Rahman, 1989). This index reflects material composition, the degree of consolidation, fracturing, and the presence/absence of fluids within pores that affect the elastic moduli. The material index is defined in terms of elastic moduli by the following equation (Abdel Rahman, 1989):

$$M_i = (1-4\sigma) \quad . \tag{7}$$

Higher values of $M_i$ represent higher material quality, while lower values indicate low material quality. Figure 16 shows the distribution of $M_i$ in the limestone bedrock.

***Concentration Index ($C_i$)*** - Bowless (1984) described the degree of material concentration or compaction by this parameter. Rock or soil compaction status is considered as a measure of the degree of material competence for foundation design and other civil engineering purposes. Bowless (1984) introduced the concentration index in terms of Poisson's ratio as follows:

$$C_i = (1+\sigma) \quad . \tag{8}$$

Higher values of the $C_i$ indicate higher material quality, while lower values indicate lower material quality. Figure 17 shows the distribution of $C_i$ in the limestone bedrock.

***Stress Ratio ($S_i$)*** - The stress ratio represents the relationship between the vertical stress at a certain depth and the horizontal stress. Stress ratio was calculated as using the following formula:

$$S_i = \sigma(1-\sigma) \quad . \tag{9}$$

Small values of $S_i$ indicate good, competent to fairly competent material. Higher values of Si indicate incompetent (very soft to soft) material (Abdel Rahman, 1991). Figure 18 shows the distribution of $S_i$ in the bedrock.

***A-Value*** - The A-value is a practical measure of material competence. It is directly related to Poisson's ratio. The A-value is expressed by the following equation:

$$\text{A-value} = \ln(k)/\ln(\rho_b) \quad , \tag{10}$$

where k is the bulk modulus and $\rho_b$ is the bulk density. High values of the A-value indicate material of lower competence and vice versa. Figure 19 shows the distribution of A-values in the bedrock.

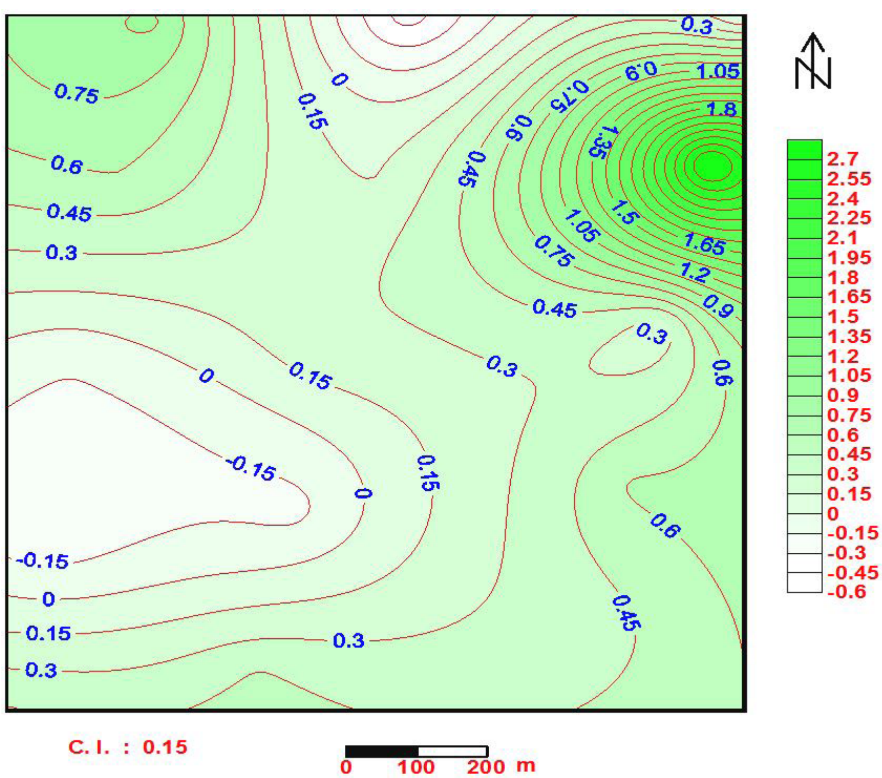


**Figure 16:** Distribution of the material index ($M_i$) for the foundation bedrock layer.

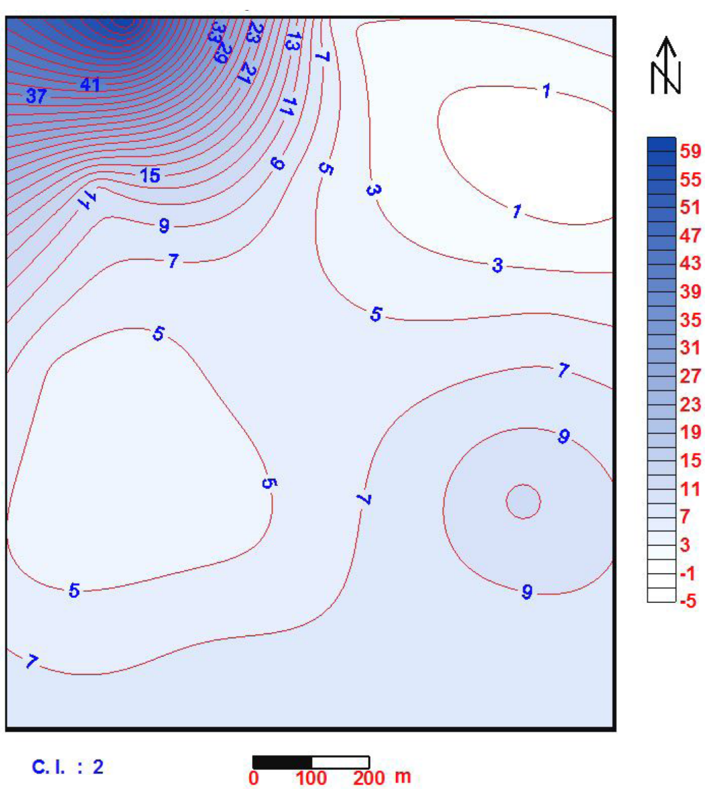


**Figure 17:** Distribution of the concentration index ($C_i$) for the foundation bedrock layer.

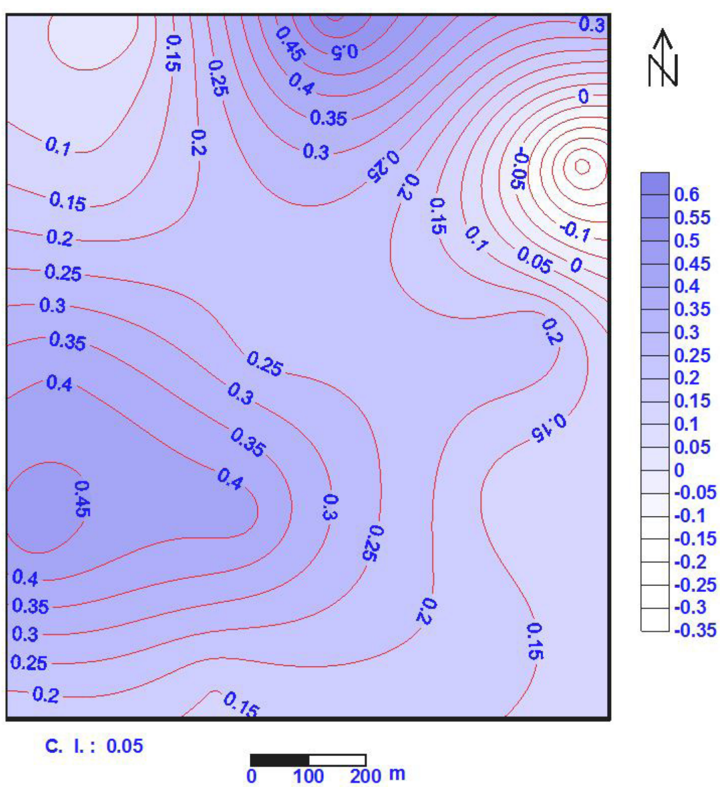


**Figure 18:** Distribution of stress ratio ($S_i$) for the foundation bedrock layer .

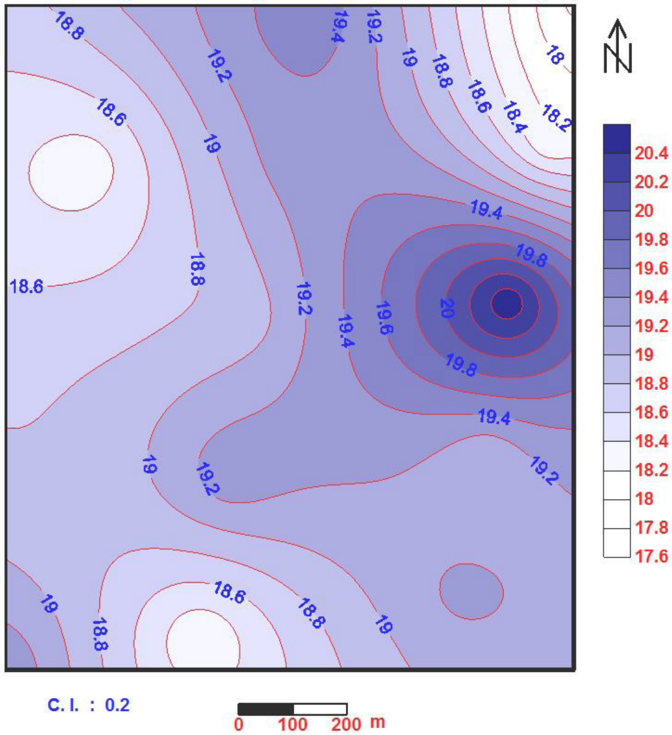


**Figure 19:** Distribution of the A-value in $cm^{-1}$ for the foundation bedrock layer.

### Foundation Material Bearing Capacities

***Ultimate Bearing Capacity ($Q_{ult}$)*** - The ultimate bearing capacity is defined as the maximum load required for shear failure or sand liquefaction. It can be derived in terms of shear wave velocity according to the following equation (Abdel Rahman, 1990):

$$Q_{ult} = 10^{2.932} (\log(V_S - 1.45)) \quad . \qquad (11)$$

Higher values of $Q_{ult}$ indicate higher material quality and lower values of $Q_{ult}$ indicate lower material quality. Figure 20 shows the distribution of $Q_{ult}$ in the bedrock.

***Allowable Bearing Capacity ($Q_a$)*** - Allowable bearing capacity ($Q_a$) is defined as the maximum load that can be attained and still avoid shear failure or sand liquefaction. It can be determined from $Q_{ult}$ assuming a suitable factor of safety F=2 for cohessionless material and F=3 for cohesive material (Parry, 1977), and can therefore be expressed as follows:

$$Q_a = Q_{ult}/F$$

The same patterns as $Q_{ult}$ map (Figure 20) are found on the $Q_a$ map (Figure 21) but values are reduced in magnitude. Higher $Q_{ult}$ or $Q_a$ values indicate low material quality.

## Comparison of Field and Laboratory Geotechnical Property Measurements

Along Profile 5, samples of limestone were taken from the bedrock, which is exposed on the surface. Some geotechnical properties of these samples were measured at the Petrophysical Studies Unit in the Faculty of Science of Ain Shams University. The geotechnical properties including Poisson's ratio, Young's modulus, rigidity modulus, bulk modulus, P- and S-wave velocities that were measured in the laboratory are shown in Table 1. It is evident from the Table 1 that some values measured in the field by shallow seismic refraction are generally close to those measured in the laboratory. Some values measured in the field are slightly lower than those measured in the laboratory because the conditions of measurement in the laboratory differ from in situ conditions.

**Table 1: Comparison Between Laboratory Values and Seismic Velocity Derived Field Measurements of Geotechnical Properties.**

| Geotechnical Properties | Laboratory Measurements | Field Measurements |
|---|---|---|
| Poisson's ratio (σ) | 0.31 | 0.3 |
| Young's modulus (E), g/cm$^2$ | 6.6 | 4.6 |
| Rigidity modulus (μ), g/cm$^2$ | 2.52 | 1.86 |
| Bulk modulus (k), g/cm$^2$ | 5.69 | 3.40 |
| P-wave velocity, m/s | 5960 | 4550 |
| S-wave velocity, m/s | 3150 | 2750 |

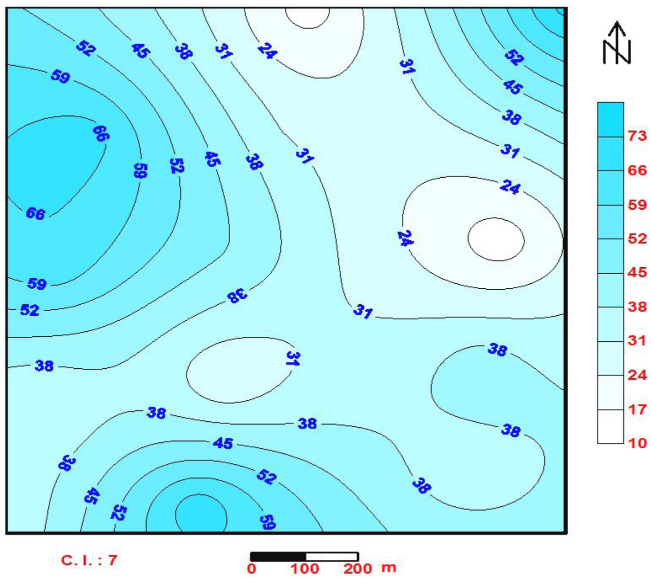


**Figure 20:** Distribution of the ultimate bearing capacity ($Q_{ult}$) in kg/cm$^2$ for the foundation bedrock layer.

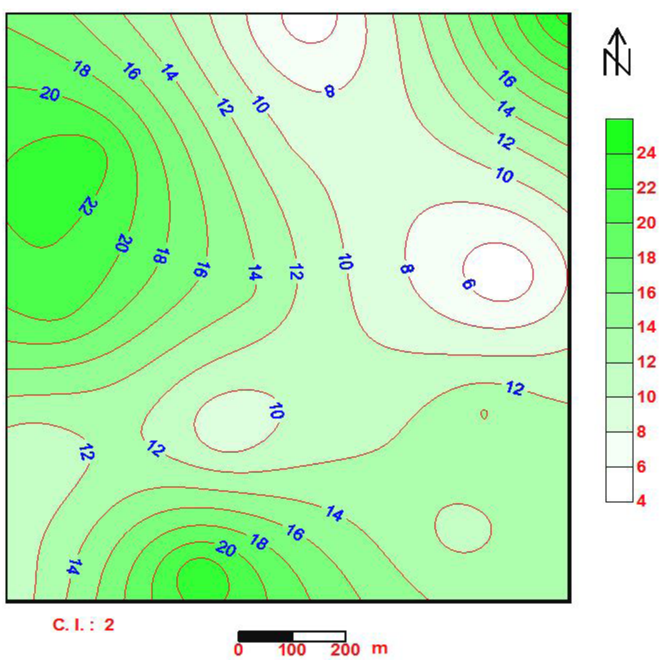


**Figure 21:** Distribution of the allowable bearing capacity ($Q_a$) in kg/cm$^2$ for the foundation bedrock layer.

## Results and Discussion

Based on the calculated values (from seismic P- and S-wave velocities) of eleven geotechnical properties for the foundation bedrock, the investigated site was divided into three zones of different competences, designated as good, fair, and weak (Figure 22). ArcGIS Version 9 (ESRI, 2005) was used for classification of these three zones . The good competence zone occupies the northwestern and southwestern parts of the study area. The fair competence zone is found within the central and eastern parts of the site while, the weak competence zone is located in the northeastern and western parts of the study area.

From this interpretation, it is evident that the weaker parts of the bedrock might be due to shear zones, faulting, fractures, joints, and zones of weathering. All of these structural features can lead to slight degrees of low competence. Locations of good competence zones and higher material quality within the bedrock are the best sites for building foundations and other civil engineering construction projects.

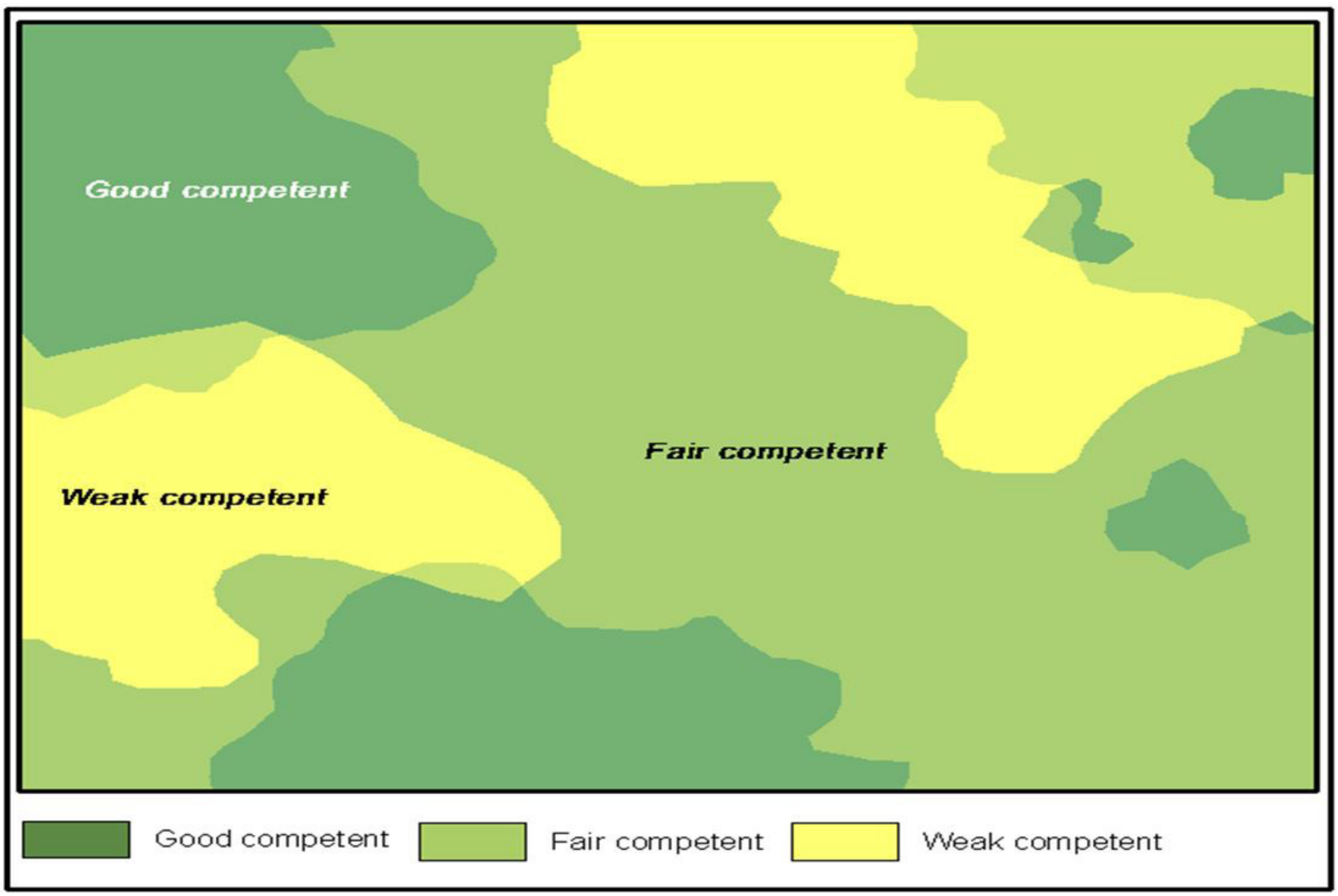


**Figure 22.** Site competence zones of bedrock in the study area.

## Acknowledgments

We wish to thank Dr. A. Saif El-Nasr and faculty members of the Assiut University Geology Department for their discussion and comments. We also appreciate the support provided by Professor R. Fat-Helbary and the staff of Aswan Research Center of Earthquakes and Professor A. El-Sayed and the staff of the Petrophysical Studies Unit of Ain Shams University.

## References

Abdel Aati, A. H. and S. H. Shabaan, 2013, Detecction of karstic limestone bedrock by shallow seismic refraction in an area west of Assiut, Middle Egypt, The Leading Edge 32, no. 3.

Abdel Aati, A. H., 1995, Geological, environmental and seismic refraction studies for site evaluation and selection of Assiut new city, Middle Egypt, 2nd Conference on Scientific and Applied Experiences of Urban Development in Upper Egypt, Faculty of Engineering, Assiut University.

Abdel Aati, A. H., 2000, Applications of geophysics in urban planning, review article (unpuplished), Assiut University.

Abdel Hakam, M. S., 2007, Geotechnical Site Studies in Hurghada City, Red Sea, Egypt, M. Sc. Thesis, Assiut University.

Abdel Rahman, M., I. Setto, and El-Werr, 1992, Inferring mechanical properties of the foundation materials at the 2nd industrial zone, Sadat city from geophysical measurements, EGS Proceedings of the 10th Annual Meeting, Cairo.

Abdel Rahman, M. 1989, Evaluation of kinetic elastic moduli of the subsurface materials and application to engineering geologic maps at Maber- Risabah area (Dahmar province), North Yemen, Egypt. J. Geol., 33.

Abdel Rahman, M., 1991, Rock material competence assessed by seismic measurements with emphasis on soil competence scales and their applications in some urban areas in Yemen, EGS proceedings of the 9 th Annual Meeting, Cairo.

Al-Kadasi, A. N.,2002, Comparative Field and Laboratory Seismo-Technical Parameters of the Foundation Rocks with Applications to Some of the New Cities in Egypt, Ph.D. thesis, Ain Shams University.

Burger, H. R., 1992, Exploration Geophysics of the Shallow Subsurface, Prentice- Hall. Inc.

Bowless, J. E., 1984, Phsical and Geotechnical Properties of Soils, McGraw-Hill

Dobrin, M. B. and C. H. Savit, 1988, Introduction to Geophysical Prospecting, McGraw-Hill, 4th edition

Environmental Sciences and Research Institute (ESRI), 2005, ArcGIS, Version 9.

Imran, M. N., 2006, Geophysical and Geotechnical Studies on the Areas around El-Madinah El-Minwara, Kingdom of Saudi Arabia, Ph.D. thesis, Assiut University.

Omara, S., M. R. El-Tahlawi and H. H. Mansour, 1970, The geology of the environs of Assiut, Bulliten of the Society of Geography,43.

RimrockGeophysics, 1995, User's guide of SIP software program.

Seisa, H. H., 1991, A Contribution to the Interpretation of Shallow Refraction Seismic Data, Ph.D. thesis, Technical University of Berlin.

Shabaan, S. H., 2008, Shallow Seismic Refraction Exploration for Engineering Site Investigations in the Area West of Assiut city, Middle Egypt, M.Sc. thesis, Assiut University.

Sjogren, B., 1984, Shallow Refraction Seismic, Chapman and Hall.

Site investigation, 2000, Egyptian Code of Soil Mechanics, Design and Construction of Foundations, HBRC, 5th edition.

Walthan, A. C., 1994, Foundations of Engineering Geology, Chapman and Hill.

Ward, S. H., 1990, Geotechnical and Environmental Geophysics, Vol.3, SEG.

Youssef, M. M., et al., 2003, Report on field trip Assiut-Kharga workshop on geoindicators and their applications in arid regions ( unpuplished), Assiut University.

Zidan, G., 1988, Geophysical and Geotechnical Study on El-Salam Suburb Area, Kharga, Egypt, M.Sc. thesis, Assiut University.

# TUNNEL DISCRIMINATION USING MOBILE GEOPHYSICAL ARRAYS

**Tomas C. Goode – MWH Global, Tempe, Arizona**
**Ty P. A. Ferré – University of Arizona, Tucson, Arizona**
**Andrew C. Hinnell –University of Arizona, Tucson, Arizona**

**Corresponding Author:**
**Tomas C. Goode, Ph.D., R.G., Senior Hydrogeologist**
**MWH Global, Inc.**
**1620 W. Fountainhead Pkwy, Suite 202**
**Tempe, Arizona 85282**
**email: Tomas.C.Goode@mwhglobal.com**

## Introduction and Background

Subsurface geophysical imaging has become a frequently used tool for a range of subsurface investigations including hydrogeologic, geotechnical, archaeological, and environmental applications. The methods for imaging are equally varied, potentially deploying electrical, electromagnetic, seismic, or gravimetric, or a combination of multiple methods. The selection of the right geophysical tool often requires some preliminary understanding of the investigation site which may include the soil conditions, the anticipated depth of investigation, and the potential features of subsurface targets of interest. Once a geophysical tool is selected, defining the appropriate configuration of measurements to interrogate and discriminate characteristics within the subsurface is the next concern. This may include the selection of measurement to confirm expected subsurface conditions or investigating unknown environments. This study presents an approach for the selection of a mobile geophysical survey for tunnel discrimination using a capacitatively-coupled resistivity (CCR) array for electrical resistivity tomography (ERT).

Capacitatively-coupled resistivity surveys are useful for locating electrically conductive metallic targets, and the strong dependence of the electrical properties of soils to water saturation, soil texture, and solute concentration, allows for detection of nonmetallic targets as well. The use of CCR has become more common in the past decade as an investigative tool for ERT because of its ease of use and rapid data acquisition; in turn providing a cost-effective, non-invasive means for evaluating large regions of the subsurface. Kuras et al. (2006) provide a detailed theoretical background and functional limitations of CCR arrays and how they relate to galvanically coupled resistivity surveys. Unlike galvanically coupled resistivity surveys which require direct contact between the electrode and the ground, CCR surveys allow the user to drag the measurement equipment along the ground surface manually or behind an all-terrain vehicle. CCR has demonstrated to be equivalent to galvanically coupled DC resistivity surveys and a valuable complement to other geophysical measurement techniques (Allred et al., 2006; Hauck and Kneisel, 2006; Kuras et al., 2007; De Pascale et al., 2008; Hickin et al., 2009). The mobility of the CCR method produces a continuous set of electrical measurements for a survey investigation,

***Keywords:*** Tunnel Discrimination, Capacitatively-Coupled Resistivity (CCR), Electrical Resistivity Tomography (ERT).

with the depth of the investigation being a function of electrode separation. When using a fixed arrangement of electrodes, subsurface image resolution is also a function of survey speed. Kuras et al. (2006 and 2007) identified that the most appropriate array style for use with CCR sensors is a dipole-dipole array. However, the key limitation in the use of the dipole-dipole array is that signal response becomes limited with large separations between current and potential dipoles (n-spacing). When considering survey speed and distance between electrodes, the selection of the appropriate CCR survey design is critical for target discrimination.

## Methods

Our goal in designing a CCR survey is to select the electrode configuration that is best able to identify a subsurface target of interest and which discriminates among differing subsurface targets of interest. Our approach intentionally avoids computationally expensive inversion; instead, we chose to direct our investigation through the use of voltage measurements to optimize our survey design. The targets being considered here are horizontal buried tunnels with circular cross sections. The selection of tunnels varies in their radius and depth; but, they have a constant electrical resistivity. They are evaluated individually, embedded in a homogeneous background with a different electrical resistivity. It is important to note that this approach may not be effective in a highly heterogeneous subsurface environment, in which case apparent resistivities and subsequent resistivity inversion may be necessary to distinguish a target from the background. Also, while we are only considering circular tunnels for these analyses, non-circular tunnels could also be considered using this same method.

Our approach uses the analytical element model described by Furman et al. (2002) to predict the response of a set of CCR measurements to isolated subsurface heterogeneities. The analytical element model is used to predict the electrical potential (voltage) that would be measured with a mobile survey of a capacitatively-coupled dipole-dipole array aligned normal to the long axis of the target tunnels (Figure 1). Measurements from increasing increments of electrode spacing (n-spacing) can be roughly interpreted as representing measurements of increasing depth as indicated in Figure 1b. The potential number of targets evaluated through this investigation is 100 (5 different r values for 20 different z values). However, only a total of 85 targets are possible given the 15 cases where a target radius is larger than its depth. For this evaluation, each tunnel has a resistivity of 10,000 ohm-m (approximating an air filled void) with a homogeneous background resistivity of 100 ohm-m, and the injected current is 1 amp. All of the analyses were developed using MATLAB (Mathworks, 2011).

## Results

The simulated response of a dipole-dipole survey moving over a single target tunnel with a radius of 1 m and a depth of 6 m is observed by plotting the voltage measurements along the course of a survey. Figure 2 displays voltage measurements for a survey using an a-spacing of 1 m and n-spacings ranging from 1 to 8. As might be expected, the signal response is generally greatest with the small n-spacings, and diminishes with larger n-spacings (having greater distance from the current source). It is also important to note that with increases in n-spacing, the distance between the current dipole and the center of the target become further off-set from the maximum signal response. In essence, the current dipole has moved further away from the target by the time the maximum signal response has been measured in the larger n-spaced dipole. This explains the increasing horizontal off-set in peak signal response for the increasing n-spacings displayed in this figure. However, we still see that the voltage response is symmetrical on both sides of the peak signal variation. Given this survey over a relatively shallow target, we also find that the peak variations in signal response are observed with the smaller n-spacings, in this case the peak signal variation appears in n-spacings 2 and 3.

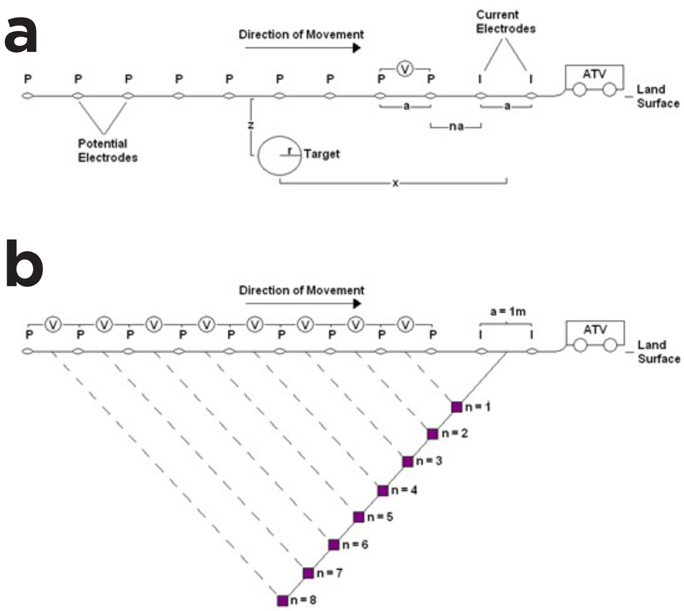


**Figure 1:** (**a**) ERT design components for a CCR dipole-dipole survey where electrodes I are current electrodes, electrodes P are potential (voltage) electrodes, a equals the spacing between electrode dipoles (pairs), z equals the depth below land surface, r equals the radius of the cylindrical subsurface target (tunnel), and x is the distance between the center of the current dipole and the center of the tunnel. The mobile survey is assumed to be moving from left to right over the tunnel. (**b**) Conceptual plotting points (roughly representative of survey penetration depths) for voltage measurements, displayed for a hypothetical mobile survey having an a-spacing of 1 m and n-spacings ranging from 1 to 8.

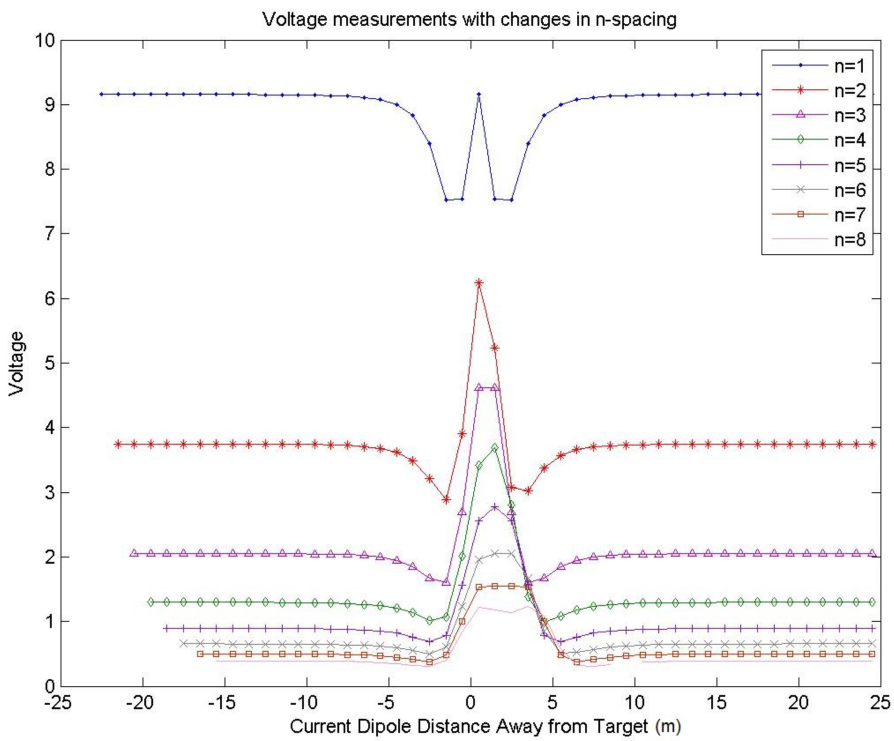


**Figure 2:** Simulated changes in voltage response associated with variations in n-spacing are plotted along the vertical axis. The horizontal axis represents the distance (in meters) between the center of the current dipole and the center of the target tunnel. Multiple measurements are made along the path of a mobile CCR survey moving from left to right across the figure. The survey assumes a fixed a-spacing of 1 m with n-spacings ranging from 1 to 8. The survey is moving across an air-filled target tunnel with a radius of 5 m and centered at a depth of 6 m. It is important to note that with increases in n-spacing, the distance between the current dipole and the center of the target become further off-set from the maximum signal response. In essence, the current dipole has moved further away from the target by the time the maximum signal response has been measured in the larger n-spaced dipole. This explains the increasing horizontal off-set in peak signal response for the increasing n-spacings displayed in this figure.

We expect that the voltage response will be variable not only to changes in dipole configuration of the mobile electrical survey, but also with changes in target size and depth. Figure 3a displays the simulated voltage measurements obtained along a survey path over a target of variable radius. In this particular case, the target depth has been fixed at 6 m, with a-spacing of the dipoles fixed at 1 m and an n-spacing of 1. The y-axis indicates differing radii of potential targets ranging from 1 to 5 m, while the x-axis displays the horizontal distance between the current dipole to the center of the target projected at the land surface. The figure displays changes in voltage with respect to changes in target radius along the horizontal path of the current dipole as the CCR survey moves from left to right. Looking from left to right, we see that voltage measurements remain relatively constant (approximately 9 volts) for most of the survey path. This voltage begins decreasing at approximately 7 m to the left of the target for the largest tunnel radius (as observed previously in Figure 2). As expected, the survey is most sensitive to the largest target from the greatest horizontal distance away from the target. Note that the peak changes in voltage are measured near the zero value in the x-axis. However, as discussed briefly above, the peak voltage becomes more "off-centered" for the larger n-spacing because the current dipole has moved further away from the target. Upon evaluating a target with a fixed radius, changes in depth show a similar behavior with regard to changes in voltage as the mobile electrical survey moves across the target. Figure 3b displays the simulated voltage measurements obtained along a survey path over a target with a radius of 5 m at depths ranging from 6 to 20 m with an a-spacing of 1 m and an n-spacing of 1.

When considering the dynamic nature of a mobile CCR survey, and the composite set of voltages obtained from the full suite of potential dipoles of variable a-spacings and n-spacings, the magnitude and variability of changes in voltage responses to individual targets may be significant across the extent of the survey. By calculating the voltage response differences between differing survey configurations with respect to specific target tunnels, we are able to develop a ***target discrimination map***, which displays tunnels within a range of r and z values that are distinguishable from a selected target tunnel. This is constructed by choosing an appropriate error level (in voltage units), then calculating the difference between survey voltage from each potential target and our selected target tunnel. This difference or threshold value may represent the expected survey noise or survey measurement uncertainty. We then identify those targets with difference less than or greater than the selected threshold. The resulting target discrimination maps for a selected target tunnel are shown in Figure 4 for three different surveys. In simple terms, the blue area surrounding the white asterisk can be thought of as the set of tunnels that cannot be discriminated from the target tunnel. The survey with a-spacing of 5 m leads to the smallest indistinguishable (blue) region in Figure 4. Moving from left to right on the panels shown, we are able to discriminate our selected target from 3.53%, 12.94%, and 60.0% of the potential number of targets. In practical terms of survey design, if a particular subsurface target of interest has been identified (approximate size and depth), along with an estimate of potential survey noise, we are able to use this process to identify which mobile survey configuration has the greatest focus on our target. Further, through the use of this process, we know that the survey dimensions were selected using a process which best discriminates our selected target from other potential targets in the subsurface.

By repeating the analyses leading to Figure 4 we are able to determine what percentage of targets (from the total of 85 targets in our evaluation) we are able to discriminate from our selected target using differing survey configurations. For each selected target tunnel, we can determine the percent of targets that are excluded using a selected survey design. The results displayed in Figure 5 can be thought of as ***target identifiability maps*** for the selected survey sets. While all of these identifiability maps indicate that both shallow and larger targets are more identifiable than smaller and deeper targets, of the panels displayed in Figure 5, a survey having an a-spacing of 5 m with n-spacings of 1 and 2 has the greatest ability to identify and discriminate targets over the broadest range of depth and size.

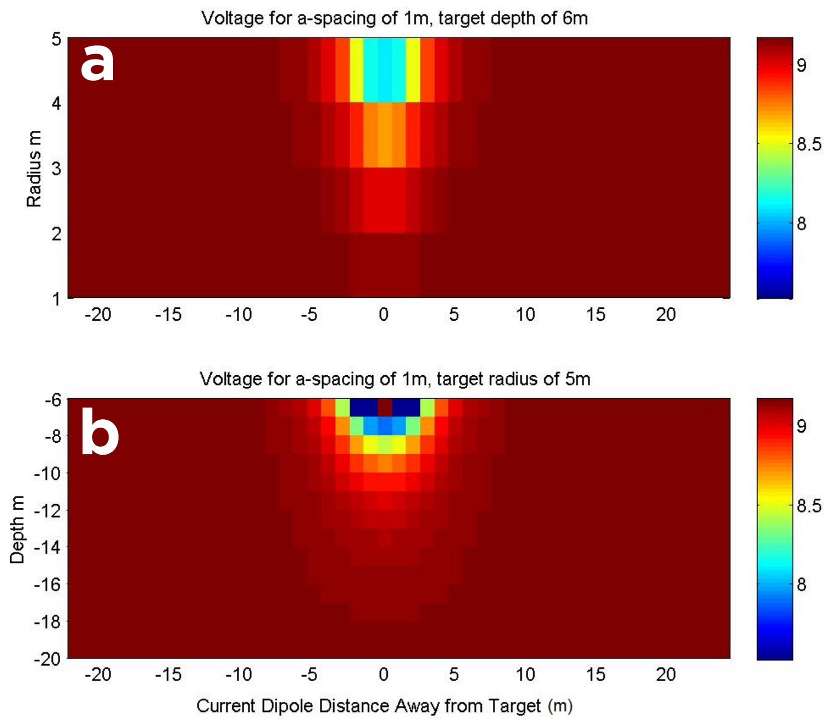


**Figure 3:** (**a**) Simulated voltage responses from a mobile CCR survey for targets having a fixed depth of 6 m and a variable radius from 1 to 5 m. Radius of the target is plotted along the vertical axis and the horizontal distance between the center of the current dipole and the center of the target tunnel is plotted along the horizontal axis. This panel represents a single distance between current and potential dipoles (a-spacing equals 1 m and n-spacing equals 1). (**b**) Simulated voltage responses from a mobile CCR survey for targets having a fixed radius of 5 m and of variable depth (6 to 20 m). Depth of the target is plotted along the vertical axis and the horizontal distance between the center of the current dipole and the center of the target tunnel is plotted along the horizontal axis. This panel also represents only a single distance between current and potential dipoles (a-spacing equals 1 m and n-spacing equals 1).

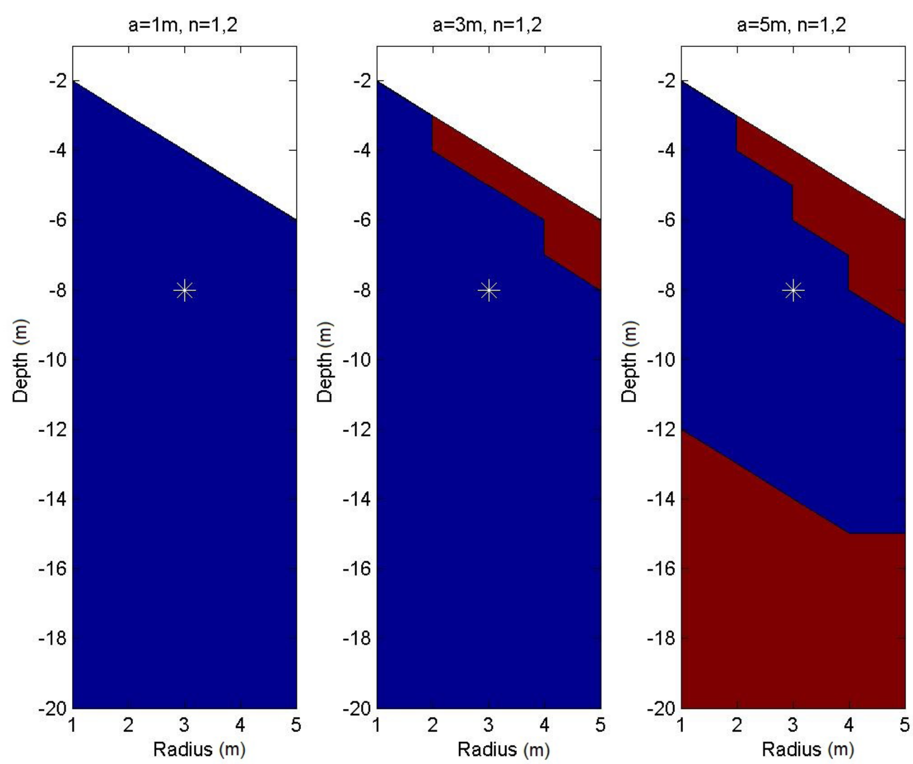


**Figure 4:** Target discrimination maps showing the tunnels that can (red) and cannot (blue) be distinguished from the target tunnel (shown with white asterisk) using the selected survey configurations for an error level of 0.4. The selected target tunnel with a radius of 3 m and a depth of 8 m is displayed on each panel with a white asterisk.

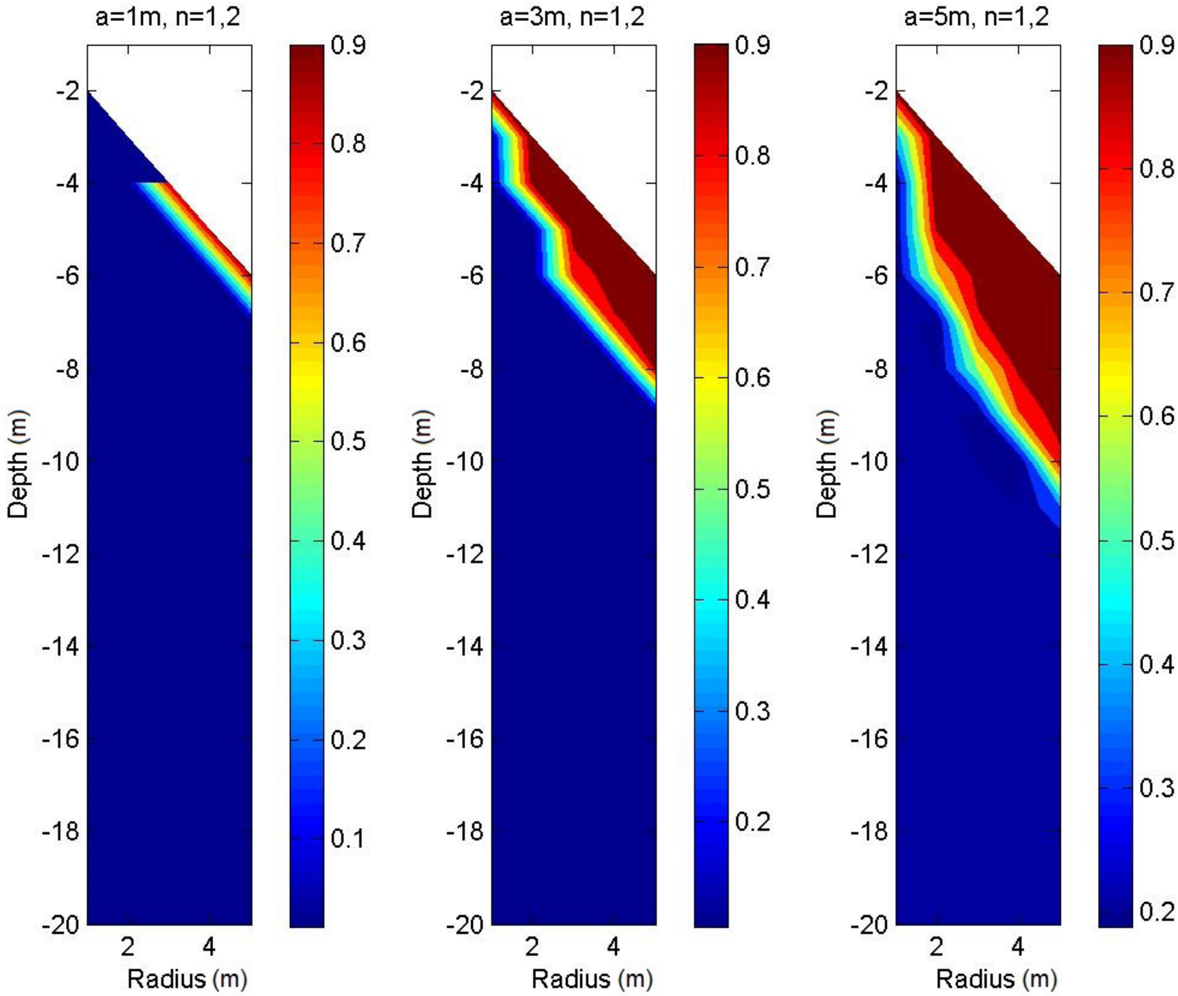


**Figure 5:** Target identifiability maps displaying the fractional discrimination for each tunnel using the selected CCR mobile array configuration.

The maps of the target discrimination maps are calculated using equally sized, symmetrical (with respect to the target tunnel location) data sets. We expect that mobile ERT surveys that have differing horizontal survey lengths, time between data measurements, and asymmetrical surveys (with respect to the target location) will have an impact on survey efficiency. For example, we find that measurements collected using the same mobile ERT survey design across the same target, but moving at differing speeds significantly impact the identifiability of target tunnels. Figure 6 displays this stepwise reduction of efficiency for the best survey design displayed in Figure 5 (a-spacing 5 m, n-spacings of 1 and 2) for speeds ranging from 1 to 8 times the original speed (2 km/hr). While we would not anticipate many CCR surveys to be conducted at 16 km/hr, we believe the concept of reduced survey efficiency as a function of speed is scalable. For a user of this process, a balance among survey speeds, target identifiability, and discrimination can be obtained to meet project goals. In these examples presented in Figure 6, we see the efficiency of our surveys continue to diminish with increasing survey speeds and that we sacrifice our ability to identify and discriminate both small, shallow targets as well as large, deep targets. Although the percentage of target discrimination at the original speed is 39.75%, it reduces to 33.08% at twice the speed, 26.02% at four times, 19.29% at six times, and 9.55% at eight times the original speed. By increasing speed, we reduce the number of measurements and in turn, reduce our ability to discriminate a selected target – regardless of array design.

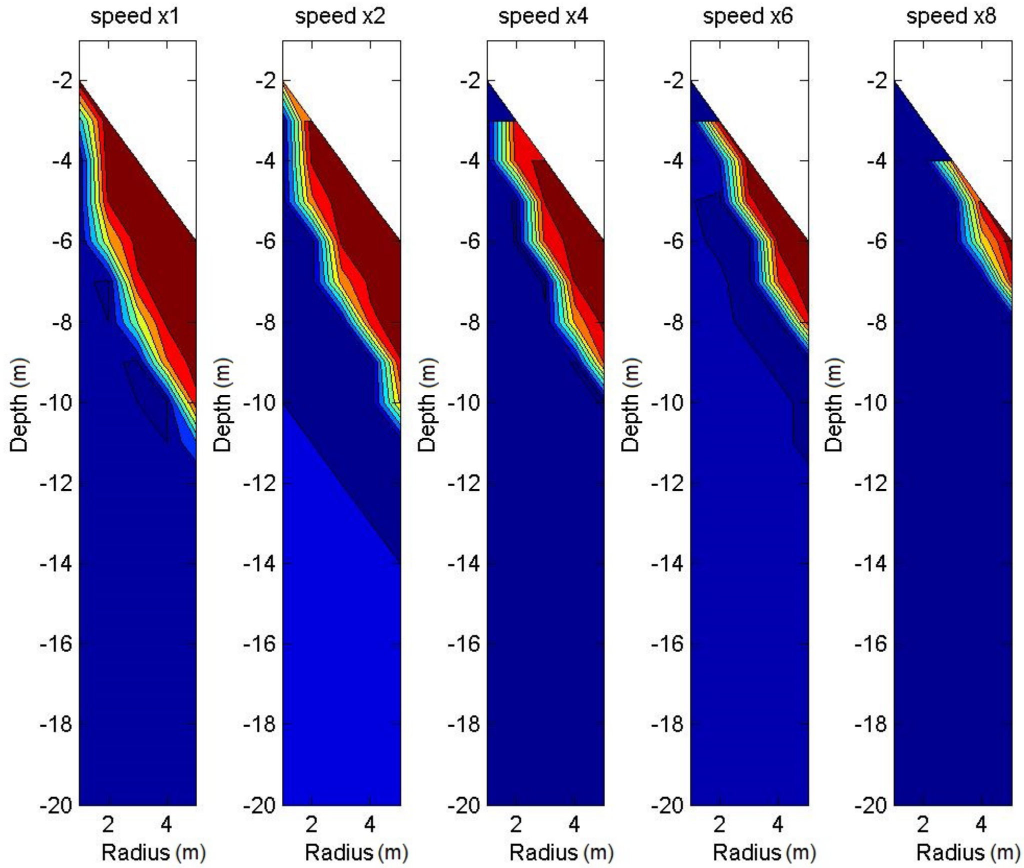


**Figure 6:** Target identifiability maps displaying the fractional discrimination for each tunnel using a CCR mobile array configuration with an a-spacing of 5 m and n-spacings of 1 and 2. However, horizontal measurement collection has been reduced incrementally by increasing the survey speed from 1 to 8 times the original survey speed (2 km/hr). The panels in this figure represent significantly reduced target discrimination as a result of increasing survey speeds.

## Conclusions

In this study, we have proposed a relatively simple approach for subsurface target discrimination using a mobile CCR survey. The approach is based on limited forward modeling of the geophysical survey response for multiple CCR survey designs. The mobile electrode arrays that were evaluated used a dipole-dipole configuration, with a-spacings ranging from 1 to 5 m, and n-spacings from 1 to 8 times the a-spacing. By evaluating different CCR survey designs and their respective measurement responses to buried tunnels of different size and depth, we have shown a means to identify and discriminate among tunnels. The method we have developed uses only the voltage measurements from the CCR survey and avoids computationally expensive inversion routines. The differences in voltage between surveys were used to create an error response surface for tunnels ranging in size from 1 to 5 m in radius, and ranging in depth from 1 to 20 m. Through the selection of an error criteria, these error response surfaces can be converted into target discrimination maps which identify tunnels that can and cannot be discriminated from a selected target tunnel. These discrimination maps may be developed by an investigator to select an appropriate CCR array design for a particular subsurface target of interest. With estimates of size, depth, and survey noise, we are able to use this process to identify which mobile survey configuration has the greatest focus on our target and which best discriminates our selected target from other potential targets in the subsurface.

The fractional discrimination for each tunnel obtained from the target discrimination maps is used to create target identifiability maps which indicate the ability for each survey to discriminate among different target tunnels. We provide an example of the potential impact of survey speed on the discrimination of target tunnels. We found a significant reduction in target discrimination with increasing survey speeds, primarily sacrificing our ability to identify small shallow targets and large deep targets. Although overall survey efficiency at the original speed is 39.75%, it reduces to 33.08% at twice the speed, 26.02% at four times, 19.29% at six times, and 9.55% at eight times the original speed. By increasing speed, we reduce the number of measurements and in turn, reduce our ability to discriminate certain targets – regardless of array design. For a user of this process, a balance can be struck among the differing components of a survey; speed, target identifiability, and discrimination can all be evaluated to meet project goals.

## References

Allred, B.J., M. Reza Ehsani, D. Saraswat, 2006. Comparison of Electromagnetic Induction, Capacitatively-Coupled Resistivity, and Galvanic Contact Resistivity Methods for Soil Electrical Conductivity Measurement, Applied Engineering in Agriculture, Vol. 22(2): 215-230.

De Pascale, Gregory P., Wayne H. Pollard, and Kevin K. Williams, 2008. Geophysical mapping of ground ice using a combination of capacitive coupled resistivity and ground-penetrating radar, Northwest Territories, Canada, Journal of Geophysical Research, Vol. 113, F02S90, doi:10.1029/2006JF000585.

Furman, A., A.W. Warrick, and T.P.A. Ferrè. 2002. Electrical potential distributions in response to applied current in a heterogeneous subsurface: solution for circular inclusions. Available at www.vadosezonejournal.org. Vadose Zone J. 1:273–280.

Hauck, Christian, and Christof Kneisel, 2006. Application of Capacitively-coupled and DC Electrical Resistivity Imaging for Mountain Permafrost Studies, Permafrost and Periglacial Process. 17: 169–177, doi: 10.1002/ppp.555.

Hickin, Adrian S., Benjamin Kerr, Thomas E. Barchyn, and Roger C. Paulen, 2009. Using Ground-Penetrating Radar and Capacitatively Coupled Resistivity to Investigate 3-D Fluvial Architecture and Grain-Size Distribution of a Gravel Floodplain in Northeast British Columbia, Canada, Journal of Sedimentary Research, v. 79, 457–477, doi: 10.2110/jsr.2009.044.

Kuras, Oliver, David Beamish, Philip I. Meldrum, and Richard D. Ogilvy, 2006. Fundamentals of the capacitive resistivity technique, Geophysics, Vol. 71, No. 3; P. G135–G152, doi:10.1190/1.2194892.

Kuras, Oliver, Philip I. Meldrum, David Beamish, Richard D. Ogilvy and Deepak Lala, 2007. Capacitive Resistivity Imaging with Towed Arrays, Journal of Environmental and Engineering Geophysics, September 2007, Volume 12, Issue 3, pp. 267–279.

MathWorks. 2011. Matlab. The MathWorks, Inc., Natick, MA.

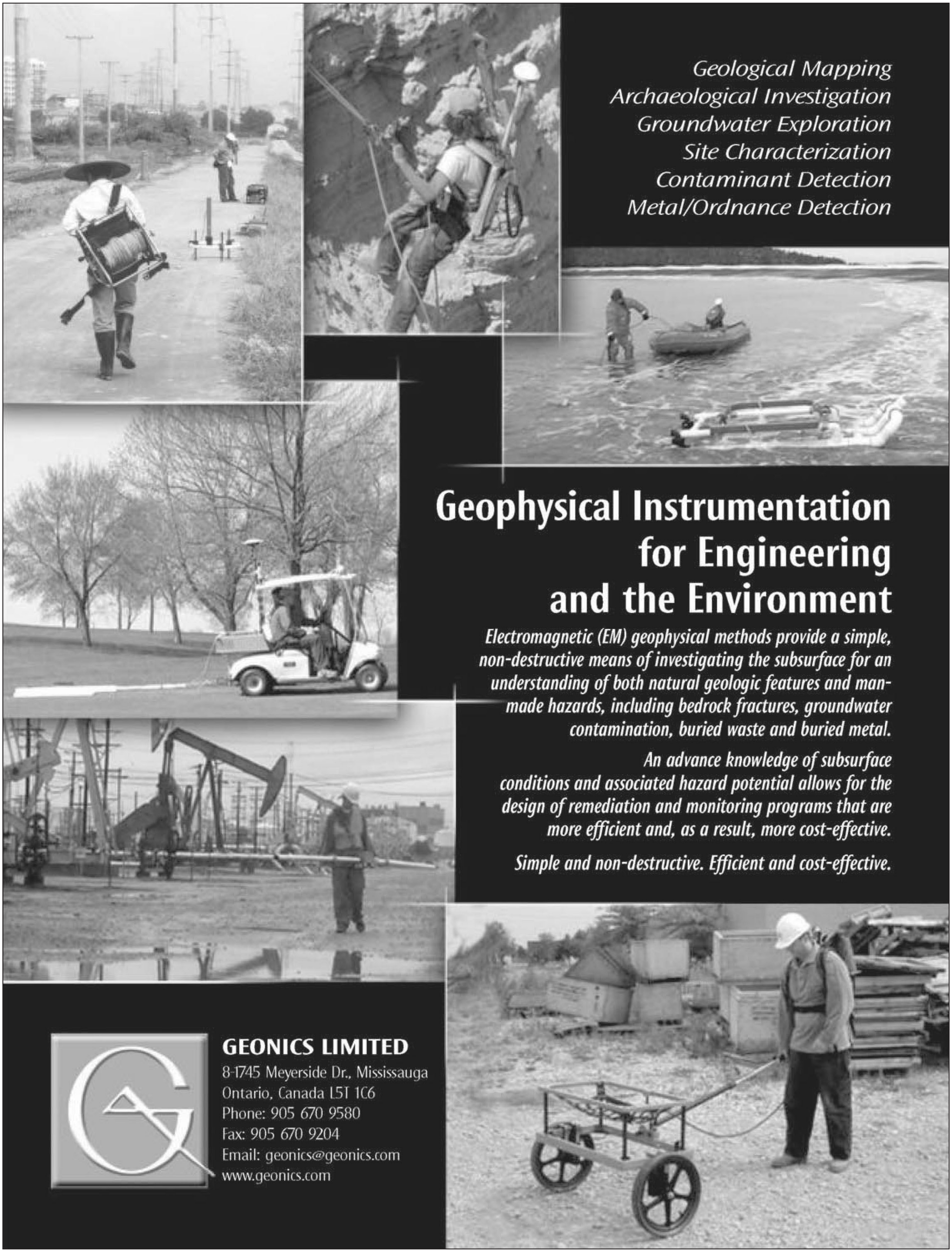
Geological Mapping
Archaeological Investigation
Groundwater Exploration
Site Characterization
Contaminant Detection
Metal/Ordnance Detection
Geophysical Instrumentation for Engineering and the Environment
Electromagnetic (EM) geophysical methods provide a simple, non-destructive means of investigating the subsurface for an understanding of both natural geologic features and man-made hazards, including bedrock fractures, groundwater contamination, buried waste and buried metal.
An advance knowledge of subsurface conditions and associated hazard potential allows for the design of remediation and monitoring programs that are more efficient and, as a result, more cost-effective.
Simple and non-destructive. Efficient and cost-effective.
GEONICS LIMITED
8-1745 Meyerside Dr., Mississauga
Ontario, Canada L5T 1C6
Phone: 905 670 9580
Fax: 905 670 9204
Email: geonics@geonics.com
www.geonics.com

Geophysical Survey Systems, Inc.

*Contact* Jami Harmon
*Telephone* 603.893.1109
*Email* harmonj@geophysical.com
*Website* www.geophysical.com

## GSSI Launches Innovative New Ground Penetrating Radar (GPR) Control Unit at GPR 2014

**Brussels, Belgium – June 30, 2014 – GSSI announced the release of SIR® 4000 ground penetrating radar (GPR) control unit at the 15th International Conference on Ground Penetrating Radar- GPR 2014, the premier conference for the GPR industry. The new controller is designed to bridge the legacy of our traditional analog antennas with our next-generation of digital offerings. Combined, this allows true versatility and flexibility by supporting a wide range of users, beginner to advanced, in numerous applications.**

**The SIR 4000 offers unique collection modules, including Quick 3D, UtilityScan, StructureScan, and Expert Mode for efficient data collection and visualization. It also incorporates advanced display methods and filtering capabilities for 'in-the-field' processing and imaging. Fully integrated, the SIR 4000 provides a 10.4 inch high definition LED display, a simple user interface, plug-and-play GPS integration, and Wi-Fi enabled data transfer functionality.**

**The SIR 4000 is designed with a number of exclusive features, including a casted aluminum chassis that offers superior temperature stability and an impact resistant design that combined, delivers a full IP 65 rated- able to withstand tough jobsite conditions. Paul Fowler, Vice President of Sales and Marketing, commented, "GSSI has been the innovator in ground penetrating radar technology since the early 1970's, when the company introduced the world's first commercial GPR system for geophysical investigation. In that regard, the SIR 4000 combines years of engineering and in-field experience. We designed it to support every existing GSSI antenna with an eye towards future digital offerings, and to provide a high-performance instrument able to withstand the rigors of field use. The release of the SIR 4000 at GPR 2014 further proves our commitment to the GPR industry and why we remain the world leader." For pricing and availability, please contact your local sales representative.**

**About GSSI:**

**Geophysical Survey Systems, Inc. is the world leader in the development, manufacture, and sale of ground penetrating radar. Our equipment is used to explore the subsurface of the earth and to non-destructively inspect our infrastructure systems. GSSI created the first commercial GPR system nearly 45 years ago and continues to provide the widest range and highest quality GPR equipment available today.**

For Immediate Release: 6.30.2014

www.geophysical.com
12 Industrial Way • Salem, NH 03079-2837
Tel: 603.893.1109 • Toll Free: 800.524.3011 • Fax: 603.889.3984


GSSI
StructureScan3D
Expert Mode
Quick3D
Last Used Settings
New Project
Playback
GSSI
START
STOP
SIR 4000

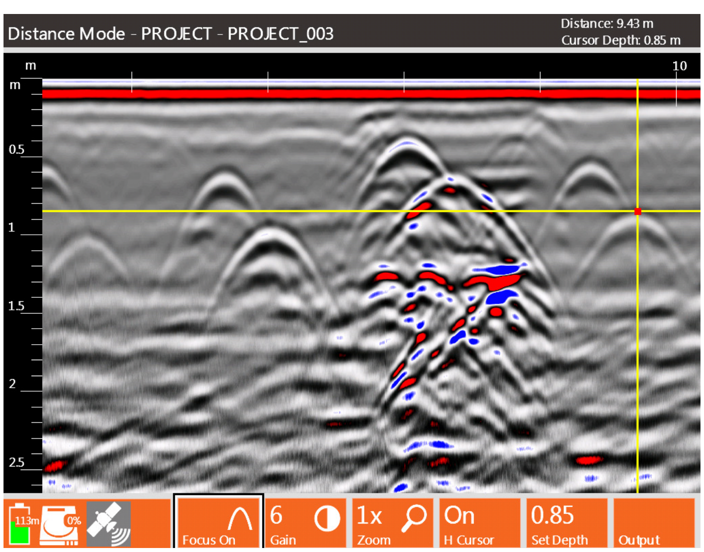
Distance Mode - PROJECT - PROJECT_003
Distance: 9.43 m
Cursor Depth: 0.85 m
m
10
m
0.5
1
1.5
2
2.5
Focus On
6 Gain
1x Zoom
On H Cursor
0.85 Set Depth
Output

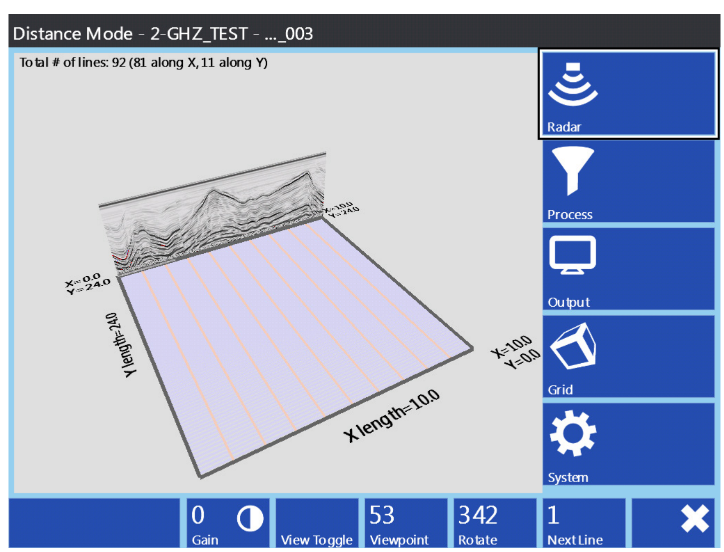
Distance Mode - 2-GHZ_TEST - ..._003
Total # of lines: 92 (81 along X, 11 along Y)
X=0.0 Y=24.0
Y length=24.0
X length=10.0
X=10.0 Y=0.0
Radar
Process
Output
Grid
System
0 Gain
View Toggle
53 Viewpoint
342 Rotate
1 Next Line

Pile Dynamics, Inc.

**Quality Assurance for Deep Foundations**

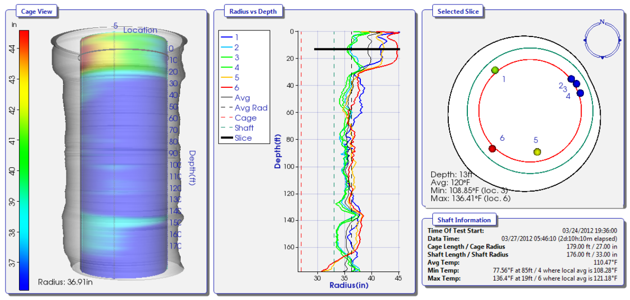


July 30, 2014

**For immediate release –**

**Thermal Integrity Profiling recognized by American Society of Civil Engineers and Deep Foundations Institute**

The American Society of Civil Engineers, ASCE, announced on July 24 the Thermal Integrity Profiler (TIP) as the 2015 winner of the Charles Pankow Award for Innovation. This Award celebrates collaboration in innovative design, materials, or construction-related research and development transferred into practice in a sustainable manner. The Award also rewards innovative approaches that help achieve at least one of the National Construction Technology Goals. The Award will be presented in March of 2015.

The innovative TIP, which uses the heat generated during cement curing to assess the shape and integrity of concrete foundations, was recognized by ASCE in part due to the collaborative efforts that were key to its development. “The thermal integrity profiling technology was developed initially at the University of South Florida (USF) where it evolved throughout three Florida Department of Transportation funded research project”, said Gray Mullins, PhD, PE, the USF Professor who led the research team. A fourth study was performed in cooperation with Washington State Department of Transportation. A joint effort was then undertaken by Foundation & Geotechnical Engineering, LLC (FGE), using the USF-licensed technology, and Pile Dynamics, Inc. (PDI). The 2 firms transformed the thermal integrity profiling technology into the Thermal Integrity Profiler.

Asked about TIP’s contributions to achieve National Construction Technology Goals, Pile Dynamics’s Garland Likins, P.E., focused on the goal of Reduction on Project Delivery Time, explaining that current test methods of evaluating the quality of cast-in-place foundation elements are performed after the concrete of the foundation has cured, a process that takes several days. Typically, construction cannot proceed until foundations are approved. An evaluation performed with TIP may yield evaluation result as early as 12 to 24 hours after concrete casting, depending on shaft diameter. This aspect is only one of the advantages of this breakthrough testing procedure. Thermal Integrity Profiling is also less labor intensive than other integrity testing methods, and examines portions of the cross sectional area of the foundation that are in the ‘’blind zone” of those other tests.

Exactly a week prior, on July 18, the Deep Foundations Institute announced that Prof. Mullins and his research team at the University of South Florida, were the recipients of the 2014 Ben C. Gerwick Award for Innovation in the Design and Construction of Marine Foundations. That honor was granted “for practical research on multiple subjects”, among them thermal integrity profiling of drilled shafts.

For more information on the Thermal Integrity Profiler please visit [www.pile.com/tip](http://www.pile.com/tip) .

30725 Aurora Road • Cleveland, Ohio 44139 USA • +1-216-831-6131 • Fax +1-216-831-0916
E-mail: info@pile.com • www.pile.com

# COMING EVENTS


The Symposium on the Application of Geophysics to Engineering and Environmental Problems (SAGEEP) provides geophysicists, engineers, geoscientists and end-users from around the world an opportunity to meet over a 5-day period to discuss near-surface applications of geophysics and learn about recent developments in near-surface geophysics.

The conference features:

| | |
|---|---|
| **A Set of Proceedings on CD and Online** | **Over 200 Oral and Poster Presentations** |
| **Special Sessions** | **Educational Short Courses & Worshops** |
| **Keynote Presentation** | **Vendor Presentations** |
| **Equipment Demonstrations** | **Commercial Exhibition** |
| **Pre-Post Conference Field Trip** | **Student and Conference Evening Events** |

Email General Chair Jeff Paine (jeff.paine@beg.utexas.edu) to add your name to an informal email list for conference details as planning progresses.

Send ideas for technical sessions, workshops, or short courses to Jeff or Brad Carr, Technical Chair (bcarr1@uwyo.edu). Session topic ideas will be accepted until September 1. Abstract submission site opens Sept. 5 - abstract deadline is slated for October 17, 2014.

| | |
|---|---|
| **Friday, August 29, 2014:** | **Session Topics due** |
| **Friday, Sept. 5, 2014:** | **Abstract site opens** |
| **Friday, October 17, 2014:** | **Abstracts deadline** |

**Save the Dates!**

**WWW.EEGS.ORG/SAGEEP 2015**

**General Chair: Jeff Paine jeff.paine@beg.utexas.edu**
**Technical Chair: Brad Carr bcarr1@uwyo.edu**

# COMING EVENTS

## Agricultural Geophysics Webinar Series

### "Using Ground Penetrating Radar for Agriculture"

The second webinar on the application of geophysics to agriculture will be offered on September 30, 2014, Tuesday afternoon, from 3:00 - 4:30 Eastern Time (2:00 - 3:30 Central Time, 1:00 - 2:30 Mountain Time, 12:00 - 1:30 Pacific Time). This second in a series of agricultural geophysics webinars will focus on the use of ground penetrating radar (GPR) in agriculture. Topics will include GPR soil water content determination, GPR use in the USDA/NRCS soil survey program, GPR forestry applications, etc. Five presenters will provide a short overviews on GPR use in agriculture during the first 30 minutes of the webinar. The last hour of the webinar will be devoted to a panel discussion with the presenters, who will answer questions from the audience. There will be no cost for participating in this webinar; however, since enrollment may be limited, participants will need to register at http://www.ag-geophysics.org (once operational in early September) in order to obtain webinar login details. One week prior to the webinar, extended versions of the presentations (approximately 20 minutes each) can be accessed via YouTube video links that will be posted at http://www.ag-geophysics.org. Participants will also have the opportunity submit questions to the presenters prior to the webinar through the http://www.ag-geophysics.org website. Those from both the geophysical and agricultural communities will benefit from this webinar and are therefore encouraged to participate.

Please contact Barry Allred (allred.13@osu.edu) if you would like more information on this upcoming agricultural geophysics webinar during the time our website is being made operational.

---

**Geophysics** and **Geology** together for **Discovery**

**ASEG-PESA 2015**

24th International Geophysica
Conference and Exhibition
**15–18 February 2015**
Perth, Western Australia

## Key Dates

**Call for Expressions of Interest in submitting an abstract:** 01 March 2014

**Call for Abstracts Opens:** 01 June 2014

**Early Bird Registration Opens:** 01 July 2014

**Call for Abstracts Closes:** 31 August 2014

**Standard Registration Opens:** 01 September 2014

**More information can be found at www.conference.aseg.org.au .**

# Call for Papers

## Special Near-Surface Geophysics in The Leading Edge

The February 2015 issue of The Leading Edge (TLE - a publication of the Society of Exploration Geophysicists) will focus on Near-Surface Geophysics. Please consider a submission to this special edition. The widespread distribution of TLE will enable a broad impact of your contribution. Your research, experience, and expertise is on the cutting edge of near-surface geophysics and is greatly welcomed and encouraged to make the Feb 2015 issue a success. The submission details and a timeline of the submission is listed below.

Oct 15: Articles due to guest editor (GE).
Oct 15 – Nov 15: GE reviews submissions.
Nov 15: GE lets authors know approved, rejected, suggestions for revision.
Nov 15 – Dec 1: Authors revise articles, return revision to GE.
Dec 1 – Dec 15: GE reviews revision, makes any final changes.
Dec 15: Revised articles due to TLE editorial staff, upload to SEG ftp site.

For more information contact: Dale Werkema (Werkema.D@epa.gov)

Environmental and Engineering Geophysical Society

**2014 Membership Application**

Renew or Join Online at www.EEGS.org

# Membership Categories

EEGS is the premier organization for geophysics applied to engineering and environmental problems. Our multi-disciplinary blend of professionals from the private sector, academia, and government offers a unique opportunity to network with researchers, practitioners, and users of near-surface geophysical methods. Memberships include access to the *Journal of Environmental & Engineering Geophysics (JEEG)*, proceedings archives of the Symposium on the Application of Geophysics to Engineering and Environmental Problems (SAGEEP), and our quarterly electronic newsletter *FastTIMES*. Members also enjoy complimentary access to SEG's technical program expanded abstracts, discounted SAGEEP registration fees, books and other educational publications. EEGS offers a variety of membership categories tailored to fit your needs. Please select (circle) your membership category below:

## Renewing Members

**Welcome back! Thank you for your continued support.**

| Category | Electronic *JEEG* Available Online | Printed *JEEG* Mailed to You |
|---|---|---|
| **Individual** | $90 | $100 |
| **Retired**<br>*Must be Approved by EEGS Board of Directors* | $50 | $100 |
| **Developing World**<br>*From Approved Countries Listed Below* | $50 | $100 |

## Introductory Members

**If you have not been a member of EEGS before, Welcome! We offer a reduced rate for new members to enjoy all the benefits of individual membership (except vote or hold office).**

| Category | Electronic *JEEG* Available Online | Printed *JEEG* Mailed to You |
|---|---|---|
| NEW! **Introductory** | $50 | $100 |

## Student Members

**Students are the future and we offer you a complimentary membership subsidized by our Corporate Sponsors. Student members enjoy all the benefits of individual membership (except to vote or hold office). Available for all students in an accredited university up to one year post-graduation. Please submit a copy of your student ID.**

| Category | Electronic *JEEG* Available Online | Printed *JEEG* Mailed to You |
|---|---|---|
| NEW! **Student** | No Cost (Membership is paid by Corporate Sponsor) | $60 |

## Corporate Members

**Corporate members enjoy all the benefits of individual membership, a corporate link on the EEGS website, a company profile in *FastTIMES*, recognition at SAGEEP and a 10% discount on advertising in *JEEG* and *FastTIMES*. Additional benefits are listed for each corporate level.**

| Category | Electronic *JEEG* Available Online | Printed *JEEG* Mailed to You |
|---|---|---|
| NEW! **Corporate Student Sponsor**<br>*Includes one (1) individual membership to EEGS and sponsors 10 student memberships* | $300 | $310 |
| **Corporate Donor**<br>*Includes one (1) individual membership to EEGS and one (1) full conference registration to SAGEEP* | $650 | $660 |
| **Corporate Associate**<br>*Includes two (2) individual memberships to EEGS, an exhibit booth and registration at SAGEEP, and the ability to insert marketing materials in the SAGEEP delegate packets* | $2400 | $2410 |
| **Corporate Benefactor**<br>*Includes two (2) individual memberships to EEGS, two (2) exhibit booths and registration at SAGEEP, and the ability to insert marketing materials in the SAGEEP delegate packets* | $4000 | $4010 |

# Membership Renewal
# Developing World Category Qualification

If you reside in one of the countries listed below, you are eligible for EEGS's Developing World membership category rate of $50.00 (or $100.00 if you would like the printed, quarterly *Journal of Environmental & Engineering Geophysics* (*JEEG*) mailed to you). To receive a printed *JEEG* as a benefit of membership, select the Developing World Printed membership category on the membership application form.

Afghanistan
Albania
Algeria
Angola
Armenia
Azerbaijan
Bangladesh
Belize
Benin
Bhutan
Bolivia
Burkina Faso
Burundi
Cambodia
Cameroon
Cape Verde
Central African Republic
Chad
China
Comoros
Congo, Dem. Rep.
Congo, Rep.
Djibouti
Ecuador
Egypt
El Salvador
Eritrea
Ethiopia
Gambia
Georgia
Ghana
Guatemala
Guinea-Bissau
GuyanaHaiti
Honduras
India
Indonesia
Iran
Iraq
Ivory Coast
Jordan
Kenya
Kiribati
Kosovo
Kyrgyz Republic
Lao PDR
Lesotho
Liberia
Madagascar
Malawi
Maldives
Mali
Marshall Islands
Mauritania
Micronesia
Moldova
Mongolia
Morocco
Mozambique
Myanmar
Nepal
Nicaragua
Niger
Nigeria
North Korea
Pakistan
Papua New Guinea
Paraguay
Philippines
Rwanda
Samoa
Sao Tome and Principe
Senegal
Sierra Leone
Solomon Islands
Somalia
Sri Lanka
Sudan
Suriname
Swaziland
Syria
Taiwan
Tajikistan
Tanzania
Thailand
Timor-Leste
Togo
Tonga
Tunisia
Turkmenistan
Uganda
Ukraine
Uzbekistan
Vanuatu
Vietnam
West Bank and Gaza
Yemen
Zambia
Zimbabwe

**1720 South Bellaire Street | Suite 110 | Denver, CO 80222-4303**
**(p) 001.1.303.531.7517 | (f) 001.1.303.820.3844 | staff@eegs.org | www.eegs.org**

Environmental and Engineering Geophysical Society

## 2014 Membership Application

Renew or Join Online at www.EEGS.org

### CONTACT INFORMATION

| Salutation | First Name | Middle Initial | Last Name |
|---|---|---|---|
| | | | |

| Company/Organization | Title |
|---|---|
| | |

| Street Address | City | State/Province | Zip Code | Country |
|---|---|---|---|---|
| | | | | |

| Direct Phone | Mobile Phone | Fax |
|---|---|---|
| | | |

| Email | Website |
|---|---|
| | |

### ABOUT ME: INTERESTS & EXPERTISE

In order to identify your areas of specific interests and expertise, please check all that apply:

| Classify Association | Classify Interest or Focus | Specific Areas of Involvement | Professional/ Scientific Societies | Willing to Serve on a Committee? |
|---|---|---|---|---|
| ☐ Consultant | ☐ Archaeology | ☐ Borehole Geophysical | ☐ AAPG | ☐ Publications |
| ☐ User of Geophysical Svcs. | ☐ Engineering | ☐ Electrical Methods | ☐ AEG | ☐ Web Site |
| ☐ Student | ☐ Environmental | ☐ Electromagnetics | ☐ ASCE | ☐ Membership |
| ☐ Geophysical Contractor | ☐ Geotechnical | ☐ Gravity | ☐ AWWA | ☐ Student |
| ☐ Equipment Manufacturer | ☐ Geo. Infrastructure | ☐ Ground Penetrating | ☐ AGU | |
| ☐ Software Manufacturer | ☐ Groundwater | ☐ Magnetics | ☐ EAGE | |
| ☐ Research/Academia | ☐ Hazardous Waste | ☐ Seismic | ☐ EER1 | |
| ☐ Government Agency | ☐ Humanitarian Geo. | ☐ Other | ☐ GeoInstitute | |
| ☐ Other | ☐ Mining | | ☐ GSA | |
| | ☐ Shallow Oil & Gas | | ☐ MGLS | |
| | ☐ UXO | | ☐ NGWA | |
| | ☐ Other | | ☐ NSG | |
| | | | ☐ SEG | |
| | | | ☐ SSA | |
| | | | ☐ SPWLA | |

1720 South Bellaire Street | Suite 110 | Denver, CO 80222-4303
(p) 001.1.303.531.7517 | (f) 000.1.303.820.3844 | staff@eegs.org | www.eegs.org

## FOUNDATION CONTRIBUTIONS

### FOUNDERS FUND

The Founders Fund has been established to support costs associated with the establishment and maintenance of the EEGS Foundation as we solicit support from larger sponsors. These will support business office expenses, necessary travel, and similar expenses. It is expected that the operating capital for the foundation will eventually be derived from outside sources, but the Founder's Fund will provide an operation budget to "jump start" the work. Donations of $50.00 or more are greatly appreciated. For additional information about the EEGS Foundation (an IRS status 501(c)(3) tax exempt public charity), visit the website at http://www.EEGSFoundation.org.

**Foundation Fund Total: $ ____________**

### STUDENT SUPPORT ENDOWMENT

This Endowed Fund will be used to support travel and reduced membership fees so that we can attract greater involvement from our student members. Student members are the lifeblood of our society, and our support can lead to a lifetime of involvement and leadership in the near-surface geophysics community. Donations of $50.00 or more are greatly appreciated. For additional information about the EEGS Foundation (a tax exempt public charity), visit the website at http://www.EEGSFoundation.org.

**Student Support Endowment Total: $ ____________**

### CORPORATE CONTRIBUTIONS

The EEGS Foundation is designed to solicit support from individuals and corporate entities that are not currently corporate members (as listed above). We recognize that most of our corporate members are small businesses with limited resources, and that their contributions to professional societies are distributed among several organizations. The Corporate Founder's Fund has been developed to allow our corporate members to support the establishment of the Foundation as we solicit support from new contributors.

**Corporate Contribution Total: $ ____________**

**Foundation Total: $ ____________**

## PAYMENT INFORMATION

- ☐ Check/Money Order
- ☐ VISA
- ☐ MasterCard
- ☐ AmEx
- ☐ Discover

**Subtotals**

**Membership: $ ____________**

**Foundation Contributions: $ ____________**

**Grand Total: $ ____________**

**Card Number** ____________ **Exp. Date** ____________

**Name on Card** ____________

**Signature** ____________

Make your check or money order in US dollars payable to: EEGS. Checks from Canadian bank accounts must be drawn on banks with US affiliations (example: checks from Canadian Credit Suisse banks are payable through Credit Suisse New York, USA). Checks must be drawn on US banks.

Payments are not tax deductible as charitable contributions although they may be deductible as a business expense. Consult your tax advisor.

Return this form with payment to: EEGS, 1720 South Bellaire Street, Suite 110, Denver, CO 80222 USA
Credit card payments can be faxed to EEGS at 001.1.303.820.3844

Corporate dues payments, once paid, are non-refundable. Individual dues are non-refundable except in cases of extreme hardship and will be considered on a case-by-case basis by the EEGS Board of Directors. Requests for refunds must be submitted in writing to the EEGS business office.

**QUESTIONS? CALL 001.1.303.531.7517**

# EEGS CORPORATE MEMBERS

## Corporate Benefactor

Your Company Here!

## Corporate Associate

Advanced Geosciences, Inc.
www.agiusa.com

Allied Associates Geophysical Ltd.
www.allied-associates.co.uk

CGG Canada Services Ltd.
www.cgg.com

Exploration Instruments LLC
www.expins.com

Geogiga Technology Corporation
www.geogiga.com

Geomar Software Inc.
www.geomar.com

Geometrics, Inc.
www.geometrics.com

Geonics Ltd.
www.geonics.com

Geophysical Survey Systems, Inc.
www.geophysical.com

Interpex Ltd.
www.interpex.com

Mount Sopris Instruments
www.mountsopris.com

Petros Eikon Incorporated
www.petroseikon.com

R. T. Clark Co. Inc.
www.rtclarck.com

Sensors & Software Inc.
www.sensoft.ca

Vista Clara Inc.
www.vista-clara.com

Zonge international, Inc
www.zonge.com

## Corporate Donor

Geomatrix Earth Science Ltd.
www.geomatrix.co.uk

Northwest Geophysics
www.northwestgeophysics.com

Spotlight Geophysical Services
www.spotlightgeo.com

## Corporate Student Sponsor

Geo Solutions Limited, Inc.
www.geosolutionsltd.com

Spotlight Geophysical Services
www.spotlightgeo.com

# EEGS STORE

Environmental and Engineering Geophysical Society

## 2014 Publications Order Form

**ALL ORDERS ARE PREPAY**

1720 S. Bellaire Street, Suite 110
Denver, CO 80222-4303
Phone: 303.531.7517; Fax: 303.820.3844
E-mail: staff@eegs.org; Web Site: www.eegs.org

**Sold To:**
Name: ______________________
Company: ______________________
Address: ______________________
City/State/Zip: ______________________
Country: ____________ Phone: ________
E-mail: ____________ Fax: ________

**Ship To (If different from "Sold To":**
Name: ______________________
Company: ______________________
Address: ______________________
City/State/Zip: ______________________
Country: ____________ Phone: ________
E-mail: ____________ Fax: ________

**Instructions:** Please complete both pages of this order form and fax or mail the form to the EEGS office listed above. Payment must accompany the form or materials will not be shipped. Faxing a copy of a check does not constitute payment and the order will be held until payment is received. Purchase orders will be held until payment is received. If you have questions regarding any of the items, please contact the EEGS Office. Thank you for your order!

**SAGEEP PROCEEDINGS**

| | | | Member | Non-Member |
|---|---|---|---|---|
| | 0036 | 2014 (CD-ROM)**NEW** | $75 | $100 |
| | 0034 | 2013 (CD-ROM) | $75 | $100 |
| | 0033 | 2012 (CD-ROM) | $75 | $100 |
| | 0030 | 2011 (CD-ROM) | $75 | $100 |
| | 0029 | 2010 (CD-ROM) | $75 | $100 |
| | 0026 | 2009 (CD-ROM) | $75 | $100 |
| | 0025 | 2008 (CD-ROM) | $75 | $100 |
| | 0023 | 2007 (CD-ROM) | $75 | $100 |

| | | | Member | Non-Member |
|---|---|---|---|---|
| | 0020 | 2006 (CD-ROM) | $75 | $100 |
| | 0018 | 2005 (CD-ROM) | $75 | $100 |
| | 0016 | 2004 (CD-ROM) | $75 | $100 |
| | 0015 | 2003 (CD-ROM) | $75 | $100 |
| | 0014 | 2002 (CD-ROM) | $75 | $100 |
| | 0013 | 2001 (CD-ROM) | $75 | $100 |
| | 0012 | 1988-2000 (CD-ROM) | $150 | $225 |
| | | SUBTOTAL—PROCEEDINGS ORDERED: | | |

**SAGEEP Short Course Handbooks**

| | | | | |
|---|---|---|---|---|
| | 0039 | 2013 Agricultural Geophysics: Methods Employed and Recent Applications - Barry Allred, Bruce Smith, et al. | $35 | $45 |
| | 0038 | 2010 Processing Seismic Refraction Tomography Data (including CD-ROM) - William Doll | $35 | $45 |
| | 0037 | 2011 Application of Time Domain Electromagnetics to Ground-water Studies – David V. Fitterman | $20 | $30 |
| | 0032 | 2010 Application of Time Domain Electromagnetics to Ground-water Studies – David V. Fitterman | $20 | $30 |
| | 0027 | 2010 Principles and Applications of Seismic Refraction Tomography (Printed Course Notes & CD-ROM) - William Doll | $70 | $90 |
| | 0028 | 2009 Principles and Applications of Seismic Refraction Tomography (CD-ROM w/ PDF format Course Notes) - William Doll | $70 | $90 |
| | 0007 | 2002 - UXO 101 - An Introduction to Unexploded Ordnance - (Dwain Butler, Roger Young, William Veith) | $15 | $25 |
| | 0009 | 2001 - Applications of Geophysics in Geotechnical and Environmental Engineering (HANDBOOK ONLY) - John Greenhouse | $25 | $35 |
| | 0011 | 2001 - Applications of Geophysics in Environmental Investigations (CD-ROM ONLY) - John Greenhouse | $80 | $105 |
| | 0010 | 2001- Applications of Geophysics in Geotechnical and Environmental Engineering (HANDBOOK) & Applications of Geophysics in Environmental Investigations (CD-ROM) - John Greenhouse | $100 | $125 |
| | 0004 | 1998 - Global Positioning System (GPS): Theory and Practice - John D. Bossler & Dorota A. Brzezinska | $10 | $15 |
| | 0003 | 1998 - Introduction to Environmental & Engineering Geophysics - Roelof Versteeg | $10 | $15 |
| | 0002 | 1998 - Near Surface Seismology - Don Steeples | $10 | $15 |
| | 0001 | 1998 - Nondestructive Testing (NDT) - Larry Olson | $10 | $15 |
| | 0005 | 1997 - An Introduction to Near-Surface and Environmental Geophysical Methods and Applications - Roelof Versteeg | $10 | $15 |
| | 0006 | 1996 - Introduction to Geophysical Techniques and their Applications for Engineers and Project Managers - Richard Benson & Lynn Yuhr | $10 | $15 |

**Miscellaneous Items**

| | | | | |
|---|---|---|---|---|
| | 0031 | Advances in Near-surface Seismology and Ground Penetrating Radar—R. Miller, J.Bradford, K.Holliger<br>Special student rate - $95.00 | $109 | $149 |
| | 0021 | Geophysics Applied to Contaminant Studies: Papers Presented at SAGEEP from 1988-2006 (CD-ROM) | $50 | $75 |
| | 0022 | Application of Geophysical Methods to Engineering and Environmental Problems - Produced by SEGJ | $35 | $45 |
| | 0019 | Near Surface Geophysics - 2005 Dwain K. Butler, Ed.; Hardcover<br>Special student rate - $71.20 | $89 | $139 |
| | 0035 | Einstein Redux: A Humorous & Refreshing New Chapter in the Einstein Saga—D.Butler | $20 | $25 |

MISCELLANEOUS ITEMS CONTINUED ON NEXT PAGE...

Publications Order Form (Page Two)

| | | | | |
|---|---|---|---|---|
| | | EEGS T-shirt (X-Large) Please circle: white/gray | $10 | $10 |
| | | EEGS Lapel Pin | $3 | $3 |
| | | SUBTOTAL—SHORT COURSE/MISC. ORDERED ITEMS: | | |

***Journal of Environmental and Engineering Geophysics*** **(JEEG) Back Issue Order Information:**
**Member Rate: $15 | Non-Member Rate: $25**

| Qt. | Year | Issue | Qt. | Year | Issue | Qt. | Year | Issue |
|---|---|---|---|---|---|---|---|---|
| | **1995** | JEEG 0/1 - July | | **2004** | JEEG 9/1- March | | **2009** | JEEG 14/1 - March |
| | | JEEG 0/2 - January | | | JEEG 9/2 - June | | | JEEG 14/2 - June |
| | **1996** | JEEG 1/1 - April | | | JEEG 9/3 - September | | | JEEG 14/3 - September |
| | | JEEG 1/2 - August | | | JEEG 9/4 - December | | | JEEG 14/4 - December |
| | | JEEG 1/3 - December | | **2005** | JEEG 10/1 - March | | **2010** | JEEG 15/1 - March |
| | **1998** | JEEG 3/2 - June | | | JEEG 10/2 - June | | | JEEG 15/2 - June |
| | | JEEG 3/3 - September | | | JEEG 10/3 - September | | | JEEG 15/3 - September |
| | | JEEG 3/4 - December | | | JEEG 10/4 - December | | | JEEG 15/4 - December |
| | **1999** | JEEG 4/1 – March | | **2006** | JEEG 11/1 - March | | **2011** | JEEG 16/1 - March |
| | | JEEG 4/2 - June | | | JEEG 11/2 - June | | | JEEG 16/2 - June |
| | | JEEG 4/3 - September | | | JEEG 11/3 - September | | | JEEG 16/3 - September |
| | | JEEG 4/4 - December | | | JEEG 11/4 - December | | | JEEG 16/4 - December |
| | **2000** | JEEG 5/3 - September | | **2007** | JEEG 12/1 - March | | **2012** | JEEG 17/1 - March |
| | | JEEG 5/4 - December | | | JEEG 12/2 - June | | | JEEG 17/2 - June |
| | **2001** | JEEG 6/1 - March | | | JEEG 12/3 - September | | | JEEG 17/3 - September |
| | | JEEG 6/3 - September | | | JEEG 12/4 - December | | | JEEG 17/4 - December |
| | | JEEG 6/4 - December | | **2008** | JEEG 13/1 - March | | **2013** | JEEG 18/1 - March |
| | **2003** | JEEG 8/1- March | | | JEEG 13/2 - June | | | JEEG 18/2 - June |
| | | JEEG 8/2 - June | | | JEEG 13/3 - September | | | JEEG 18/3 - September |
| | | JEEG 8/3 - September | | | JEEG 13/4 - December | | | JEEG 18/4 - December |
| | | JEEG 8/4 - December | | | | | **2014** | JEEG 19/1 - March |
| | | | | | | | | JEEG 19/2 - June |
| **SUBTOTAL—JEEG ISSUES ORDERED** | | | | | | | | |

| | |
|---|---|
| SUBTOTAL - SAGEEP PROCEEDINGS ORDERED | |
| SUBTOTAL - SHORT COURSE / MISCELLANEOUS ITEMS ORDERED | |
| SUBTOTAL - JEEG ISSUES ORDERED | |
| CITY & STATE SALES TAX (If order will be delivered in the Denver, Colorado—add an additional 7.62%) | |
| SHIPPING & HANDLING (US—$10; Canada/Mexico—$20; All other countries: $45) | |
| **GRAND TOTAL:** | |

Order Return Policy: Returns for credit must be accompanied by invoice or invoice information (invoice number, date, and purchase price). Materials must be in saleable condition. Out-of-print titles are not accepted 180 days after order. No returns will be accepted for credit that were not purchased directly from EEGS. Return shipment costs will be borne by the shipper. Returned orders carry a 10% restocking fee to cover administrative costs unless waived by EEGS.

**Payment Information:**

☐ Check #: ______________________________ (Payable to EEGS)

☐ Purchase Order: ______________________________
(Shipment will be made upon receipt of payment.)

☐ Visa ☐ MasterCard ☐ AMEX ☐ Discover

**Important Payment Information**: Checks from Canadian bank accounts must be drawn on banks with US affiliations (example: checks from Canadian Credit Sulsse banks are payable through Credit Sulsse New York, USA). If you are unsure, please contact your bank. As an alternative to paying by check, we recommend sending money orders or paying by credit card.

Card Number: ______________________________

Cardholder Name (Print): ______________________________

Exp. Date: ______________________________

Signature: ______________________________

Environmental and Engineering Geophysical Society

1720 S. Bellaire Street, Suite 110
Denver, CO 80222-4303
Phone: 303.531.7517
Fax: 303.820.3844
E-mail: staff@eegs.org
Web Site: www.eegs.org

# 2014 Merchandise Order Form

**ALL ORDERS ARE PREPAY**

**Sold To:**

Name: ______________________________
Company: ______________________________
Address: ______________________________
City/State/Zip: ______________________________
Country: ______________ Phone: ______________
E-mail: ______________ Fax: ______________

**Ship To** (If different from "Sold To")**:**

Name: ______________________________
Company: ______________________________
Address: ______________________________
City/State/Zip: ______________________________
Country: ______________ Phone: ______________
E-mail: ______________ Fax: ______________

**Instructions:** Please complete this order form and fax or mail the form to the EEGS office listed above. Payment must accompany the form or materials will not be shipped. Faxing a copy of a check does not constitute payment and the order will be held until payment is received. Purchase orders will be held until payment is received. If you have questions regarding any of the items, please contact the EEGS Office. Thank you for your order!

## Merchandise Order Information:

| ITEM DESCRIPTION | QTY | T-SHIRT COLOR WHITE/GRAY | MEMBER RATE | NON-MEMBER RATE | TOTAL |
|---|---|---|---|---|---|
| EEGS Mug | | | $10 | $10 | |
| T-shirt (Medium) | | | $10 | $10 | Sold Out |
| T-shirt (Large) | | | $10 | $10 | Sold Out |
| T-shirt (X-Large) | | | $10 | $10 | |
| T-shirt (XX-Large) | | | $10 | $10 | Sold Out |
| EEGS Lapel Pin | | | $3 | $3 | |

**SUBTOTAL – MERCHANDISE ORDERED:**

**TOTAL ORDER:**

| | |
|---|---|
| SUBTOTAL – Merchandise Ordered: | |
| STATE SALES TAX: (If order will be delivered in Colorado – add 3.7000%): | |
| CITY SALES TAX: (If order will be delivered in the City of Denver – add an additional 3.5000%): | |
| SHIPPING AND HANDLING (US - $7; Canada/Mexico - $15; All other countries - $40): | |

**GRAND TOTAL:**

**Payment Information:**

☐ Check #: ______________ (Payable to EEGS)

☐ Purchase Order: ______________
(Shipment will be made upon receipt of payment.)

☐ Visa ☐ MasterCard ☐ AMEX ☐ Discover

Card Number: ______________ Cardholder Name (Print): ______________

Exp. Date: ______________ Signature: ______________

Three easy ways to order:
Fax to: 303.820.3844
Internet: www.eegs.org
Mail to: EEGS
1720 S. Bellaire St., #110
Denver, CO 80222-4303

**THANK YOU FOR YOUR ORDER!**

Order Return Policy: Returns for credit must be accompanied by invoice or invoice information (invoice number, date, and purchase price). Materials must be in saleable condition. Out-of-print titles are not accepted 180 days after order. No returns for credit will be accepted which were not purchased directly from EEGS. Return shipment costs will be borne by the shipper. Returned orders carry a 10% restocking fee to cover administrative costs unless waived by EEGS.

EEGS/Forms/Merchandise Order Form/2014 Prices and details on this form are as accurate as possible, but are subject to change without notice.